This is to certify that the
thesis entitled

A HIGHLY SENSITIVE SEX DETERMINATION ASSAY FOR
LOW QUALITY DNA

presented by

BRIANNE MICHELLE KILEY

has been accepted towards fulfillment
of the requirements for the

M.S. degree in Forensic Sciences

Major Professor's Signature

3/4/09

Date

PLACE IN RETURN BOX to remove this checkout from your record.
TO AVOID FINES return on or before date due.
MAY BE RECALLED with earlier due date if requested.

DATE DUE	DATE DUE	DATE DUE

A HIGHLY SENSITIVE SEX DETERMINATION ASSAY FOR LOW QUALITY DNA

By

Brianne Michelle Kiley

A THESIS

Submitted to
Michigan State University
in partial fulfillment of the requirements
for the degree of

MASTER OF SCIENCE

Forensic Sciences

2009

ABSTRACT

A HIGHLY SENSITIVE SEX DETERMINATION ASSAY FOR LOW QUALITY DNA

By

Brianne Michelle Kiley

The sex of an individual is one of the most important attributes when developing a physical profile for a forensic investigation. Current molecular sexing techniques work well with high quality samples; however, when analyzing challenging samples, such as ancient skeletal remains or tissue with little DNA, a more sensitive sexing method is required. To represent the standard molecular sexing technique, the single copy amelogenin gene on the X and Y chromosomes was amplified using SYBR® Green real-time PCR. In a comparative assay, DYZ1, a high copy repetitive element on the Y chromosome, was multiplexed with the Ya5 Alu repetitive sequence as a human and female control, and amplified using TaqMan® technology. The sensitivity and accuracy of each method were compared by analyzing both high molecular weight and artificially degraded DNA, along with low quality DNA extracted from hair shafts and ancient skeletal remains. The DYZ1/Alu assay was successful using as little as 0.0623 pg of high molecular weight DNA, whereas the amelogenin assay required 1500 times more DNA. Further, the DYZ1/Alu assay required even less artificially degraded DNA for a positive result, the exact opposite finding using amelogenin. The DYZ1/Alu assay correctly sexed 28 of 30 hair shafts and yielded sexing results for all 41 bones, while the amelogenin assay correctly sexed 16 of 30 hair shafts and yielded sexing results for only 12 of 41 bones. Ultimately, the DYZ1/Alu assay proved to be a far more sensitive and accurate sexing technique than the standard amelogenin sexing method.

ACKNOWLEDGEMENTS

I would first like to thank my advisor, Dr. David Foran, for his guidance and support throughout my research and graduate education at Michigan State University. The opportunities and experiences he has provided will benefit my professional career greatly. I would also like to acknowledge Dr. Todd Fenton and Dr. Vincent Hoffman for sitting on my thesis committee and providing excellent advice for my project. In addition, thanks goes to Carrie Jackson for her previous work on this assay and Elizabeth Graffy, Christina Rauzi, and Stephanie Rennick for the DNA they extracted from hair and bone. Without their work, my research would not have been nearly as successful. For their support and uplifting attitudes, I would like to thank my fellow graduate students in the Michigan State University Forensic Sciences Program.

Finally, I would especially like to thank my family, friends and Adam Gobeski. Without their love, support, and patience, none of this would have been possible.

TABLE OF CONTENTS

LIST OF TABLES

LIST OF FIGURES

INTRODUCTION

Identifying the sex of unknown persons can be extremely important in a forensic investigation and is often the first step in creating a physical profile of an individual. Currently, anthropological and molecular sexing techniques work well with high quality material; however, when faced with challenging samples, these techniques can become inadequate. Anthropological sex estimation works well with full adult skeletal remains, but in other instances, sex estimation can be unreliable. Furthermore, most molecular sexing techniques target one location in the genome and work best with larger amounts of high quality DNA. Unfortunately, when DNA is both low in quality and quantity, as from aged bone or hair shafts, single copy loci may not be sensitive enough for sex determination. On the other hand, using an assay sensitive enough to detect low copy number (LCN) and poor quality DNA, sex can potentially be determined from otherwise challenging sources.

Current Sexing Techniques used in Forensic Laboratories

Anthropological Sexing Techniques

Anthropological analysis is the most common method for sexing skeletal remains. Without the estimation of sex, other characteristics, such as age and ancestry, are difficult to determine (Kimmerle et al. 2008). Typically, the sexually dimorphic characteristics of bones, most commonly from the pelvis and the skull, are utilized. However, difficulties can arise that make estimating sex challenging. For example, Kornar and Potter (2007) found that the probability of obtaining an accurate profile, including sex estimations, decreases from 89% to 58% when less than 50% of a skeleton is available for analysis. Similarly, subadult remains are difficult to sex. Even though adult sexual morphological differences are present in juveniles, they are not fully developed, making sex estimates unreliable (Cox and Mays, 2000). In addition, Kimmerle et al. (2008) discussed that biological differences in general robustness, sexual dimorphism, and stature vary among populations and can lead to unreliable estimations of sex.

Molecular DNA Analysis and Sexing Techniques

When anthropological estimations become unreliable, molecular sexing techniques can be implemented. Forensic biologists analyze DNA, generally from body fluids, hair, tissues, and touch samples, to form a DNA profile for forensic casework, missing persons, parentage testing, DNA databasing, and mass disaster victim identification (Butler, 2007). Sex is often determined by detecting the amelogenin gene on the X and Y chromosomes. The most common amelogenin sex test was developed by Sullivan et al. (1993) in which homologous regions of the gene are targeted on the X and Y chromosomes; however, the sequence on the X chromosome is 6 basepairs (bp) shorter than the Y chromosome sequence. Therefore, since females only have X chromosomes, one product of 106 bp will be observed. Conversely, males, with both an X and Y chromosome, produce 106 bp and 112 bp products respectively.

Alternative Molecular Sexing Techniques

Modifications to Amelogenin Amplification

The amelogenin gene was first sequenced by Nakahori et al. (1991). The X chromosome amelogenin gene is 2872 bp long and is located at p22, while the Y chromosome amelogenin gene, located at 11p12.2, is 3272 bp long (Nakahori et al. 1991; Haas-Rochholz and Weiler, 1997). There are 19 homologous regions of the amelogenin gene on the two chromosomes; however, differences between them include 5 deletions on the X gene ranging from 1 to 6 bp in length, and 5 deletions on the Y gene, ranging from 1 to 183 bp in length (Haas-Rochholz and Weiler, 1997).

In addition to the Sullivan et al. (1993) amelogenin sexing technique, additional sexing methods have been developed that utilize alternative amelogenin regions. Nakahori et al. (1991) were the first to describe an assay that targeted a 177 bp insertion on the X chromosome. Bailey et al. (1992) assayed the first intron of the amelogenin gene, producing a 542 bp product for the X-chromosome and a 358 bp product for the Y chromosome. Similarly, Faerman et al. (1995) created a technique specific for the 189 bp deletion on the first intron of the Y-chromosome.

Molecular Sex Determination Targeting Different Loci

Additional molecular sexing techniques have been developed that are specific for non-amelogenin sequences. For example, the zinc finger regions on the X and Y chromosomes are identical in size, but differ in sequence. A restriction digest with the enzyme Hae III digests the X and Y zinc finger sequences at different positions on each chromosome. When separated by gel electrophoresis, a zinc finger sequence in females has two bands present, while a male zinc finger sequence has four bands (Reynolds and Varlaro, 1996; Stack and Witt, 1996). In addition, Witt and Erickson (1989) developed a sex assessment assay targeting alphoid satellite DNA, consisting of highly repetitive, non-coding sequences located in the pericentromeric regions on the X and Y chromosome. This assay targeted a 130 bp sequence of alphoid satellite DNA on the X chromosome and a 170 bp sequence on the Y chromosome. Similarly, the sex determining region Y (SRY) gene has also been utilized for sex assessment (Bartha et al. 2003).

Challenges with Molecular Sex Determination

Most molecular sexing techniques, including those detailed above, require less than 1 ng of DNA; however to increase amplification signal, larger amounts of DNA are generally used (Nesser and Liechti-Gallati, 1995). Unfortunately, forensic evidence, such as fingerprints, shed hair, aged bone and teeth, often contain scarce quantities of DNA that limits analysis (Andréasson and Allen, 2003), making these techniques insufficient for sex determination. In addition, molecular sexing techniques are affected by DNA degradation. DNA degrades both biologically and chemically by hydrolysis and oxidation, creating difficulties in its analysis (Poinar, 2003). Environmental factors, such as humidity, temperature, and pH can influence the degradation process (Burger et al. 1999; Poinar, 2003). Because degradation lowers the quality of DNA, assaying a single copy locus or large DNA sequences can be difficult, since an intact copy of the desired sequence may no longer be available. This can be very problematic in molecular sexing methods, as failure to detect the Y chromosome will result in erroneously typing a sample as female.

Targeting Multicopy Loci for Sex Determination

The molecular sexing methods detailed above all assay single copy loci, thus are susceptible to being missed if very small amounts of DNA are being analyzed. Budowle et al. (2001) explained that with fewer copies of DNA template, stochastic effects can occur, resulting in the exclusion of a target locus. Stochastic effect can cause inconsistent detection of a single copy locus when sexing low quantities of DNA, thereby making sex determination unreliable.

When testing small amounts of DNA, overcoming stochastic effects can potentially be achieved by assaying high copy loci. Unlike single copy loci, multicopy loci provide a more abundant template for DNA analysis, thereby increasing the chance of obtaining the desired product. The most abundant repetitive element in human DNA is the Alu sequence, found on every chromosome. Alu repeats make up 6 – 13% of the human genome, with an estimated 500,000 to 1,000,000 copies (Mighel et al. 1997). These repeats are primate specific and make an excellent target for identifying human DNA (Mighel et al. 1997). The Alu sequence is approximately 280 bp long and is made up of two similar monomers connected by an adenine rich region (Mighel et al. 1997). The Promega Corporation developed a DNA quantification technique that utilizes the Alu repetitive regions, the AluQuant™ Human DNA Quantitiation System, which quantifies human DNA to quantities as low as 100 pg (approximately 20 cells worth) (Mandrekar et al. 2001). Similarly, Nicklas and Buel (2003) utilized a specific subfamily (Ya5) of the

Alu sequence for human DNA quantification. By targeting the Ya5 subfamily, the assay quantified human DNA down to 1 pg, 100 times more sensitive than the AluQuant™ method.

Repetitive Sequences on the Y Chromosome

High copy loci are also available on the Y chromosome that are ideal for sensitive sex determination assays. Sixty percent of the Y chromosome is comprised of long repetitive sequences, with only a small number of functional genes (Roewer et al. 1992). The DYZ family, numbered in order of frequency, makes up most of the repetitive elements on the Y chromosome, with the approximate locations for each displayed in Figure 1. DYZ1 and DYZ2 are 3.4 kb and 2.4 kb repeated sequences, respectively, located on the long arm of the Y chromosome (Roewer et al. 1992; Rahman et al. 2004). DYZ3 is a block of alphoid satellite DNA positioned on the centromeric region of the Y chromosome and is 5.7 kb long with 170 bp repeating subunits (Tyler-Smith et al. 1988). On the short arm of the Y chromosome are blocks of low repetitive sequence blocks called DYZ4 and DYZ5 (Roewer et al. 1992). These sequences have been assayed for male identification. For example, Nicklas and Buel (2006) utilized the DYZ5 repeat sequence for male DNA quantification in which 15 – 50 copies of a 137 bp repeat within the sequence was targeted. In addition, Rahman et al. (2004) assayed the 2000 – 4000 copies of the DYZ1 repetitive element for sex determination and diagnostic studies of the Y chromosome.

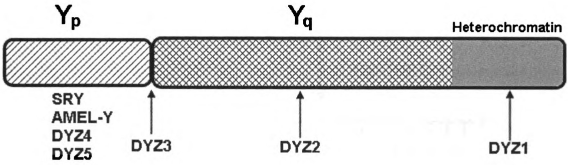

Figure 1: Location of Repetitive Elements on the Y Chromosome
A diagram of the Y chromosome with the approximate location of SRY, amelogenin (AMEL-Y), and the DYZ family of repetitive elements. The SRY, AMEL-Y, DYZ1 and DYZ5 are located on the short arm (Yp). DYZ3 is located in the centromeric region of the Y chromosome and illustrated with the arrow. DYZ1 and DYZ2 are located on the long arm (Yq). The grey box indicates the heterochromatin region on the long arm of the Y chromosome.

Real-Time Polymerase Chain Reaction

The polymerase chain reaction (PCR) is a process by which a specific region of DNA is copied (doubled) over and over, which after 30 repetitions, can turn one copy of DNA into a billion (Saiki et al. 1988) (Figure 2). PCR is initiated by the denaturing step in which the starting (template) DNA is separated into two strands. The temperature is lowered and complementary primers anneal to the DNA, flanking the DNA sequence to be studied. This is followed by enzymatic extension of the primers using a DNA polymerase extending and free nucleotides, thereby creating a copy of the desired region, termed an amplicon.

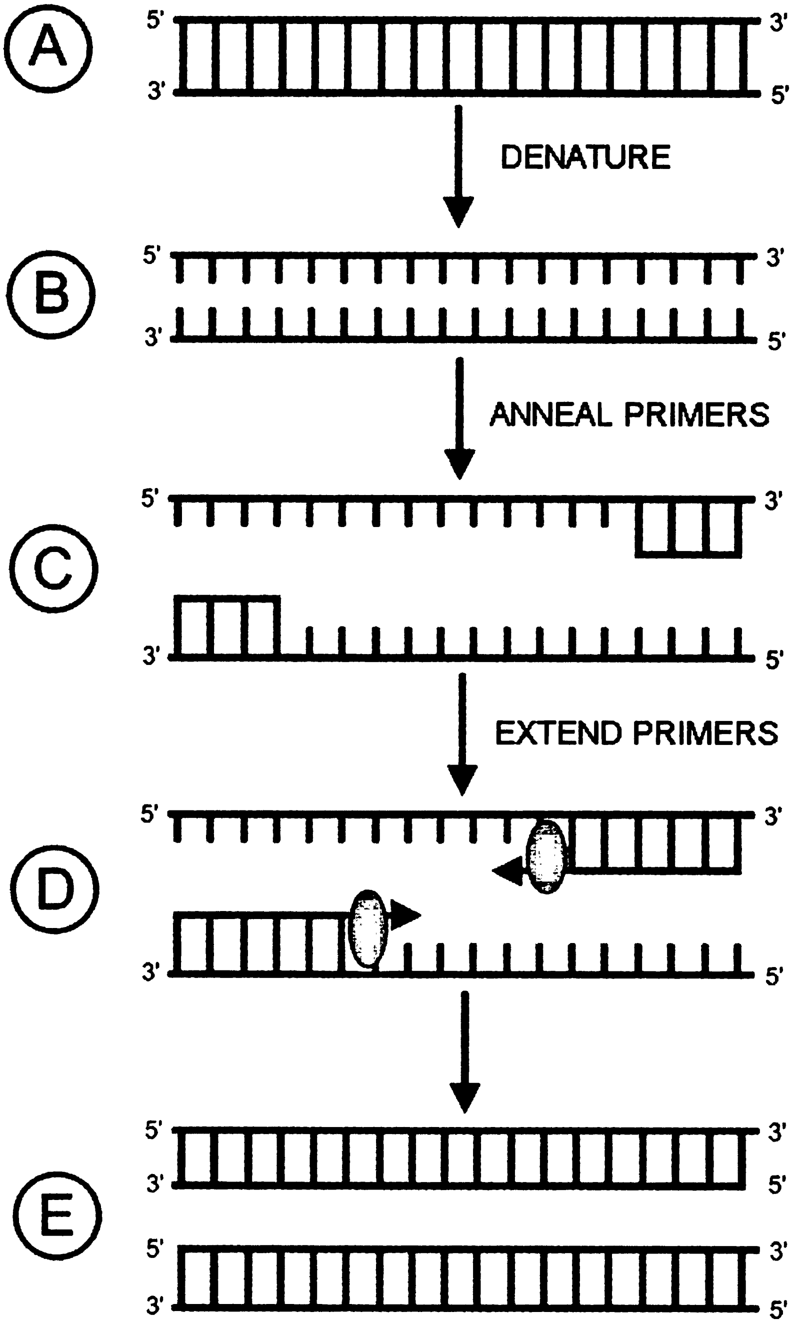

Figure 2: Diagram of the Polymerase Chain Reaction
(A) Double stranded template DNA is denatured (B) and becomes single stranded. (C) Complementary primers anneal to the template DNA. (D) DNA polymerase (oval) extends the primers resulting in (E) a copy of the desired DNA sequence. This cycle is repeated several times to create billions of copies of the target DNA sequence.

To monitor the amount of DNA being amplified during PCR, a process called real-time PCR (rtPCR) can be implemented. Several rtPCR strategies (detailed below) exist that utilize different types of fluorescent dyes to monitor DNA amplification; however, all are based on the same principles. During rtPCR, a laser is used to excite the dyes, creating a fluorescent signal. This signal is monitored by a camera within the rtPCR detection system, which then displays the signal on an amplification plot, (Figure 3). The detected signal is measured in relative fluorescent units (RFUs) and plotted against the number of PCR cycles.

During the early cycles of rtPCR, before a large amount of desired product has been produced, a certain amount of background noise can be observed. Therefore, a threshold RFU value is determined that sits above the background activity. The relationship of the amplification curve to the threshold can be utilized as a qualitative pass/fail test: if the signal crosses the threshold, then product DNA was present. The cycle in which the product signal crosses the threshold is called the cycle threshold (Ct) value. The Ct value can be used to quantify the amount of DNA present in the PCR reaction; the more DNA present, the earlier the amplification can be measured, resulting in a lower Ct value. This value can also be used to directly compare two or more DNA samples (which has more of the target sequence), or compare Ct values of known amounts of DNA to get an actual measure of the quantity of DNA product in a reaction.

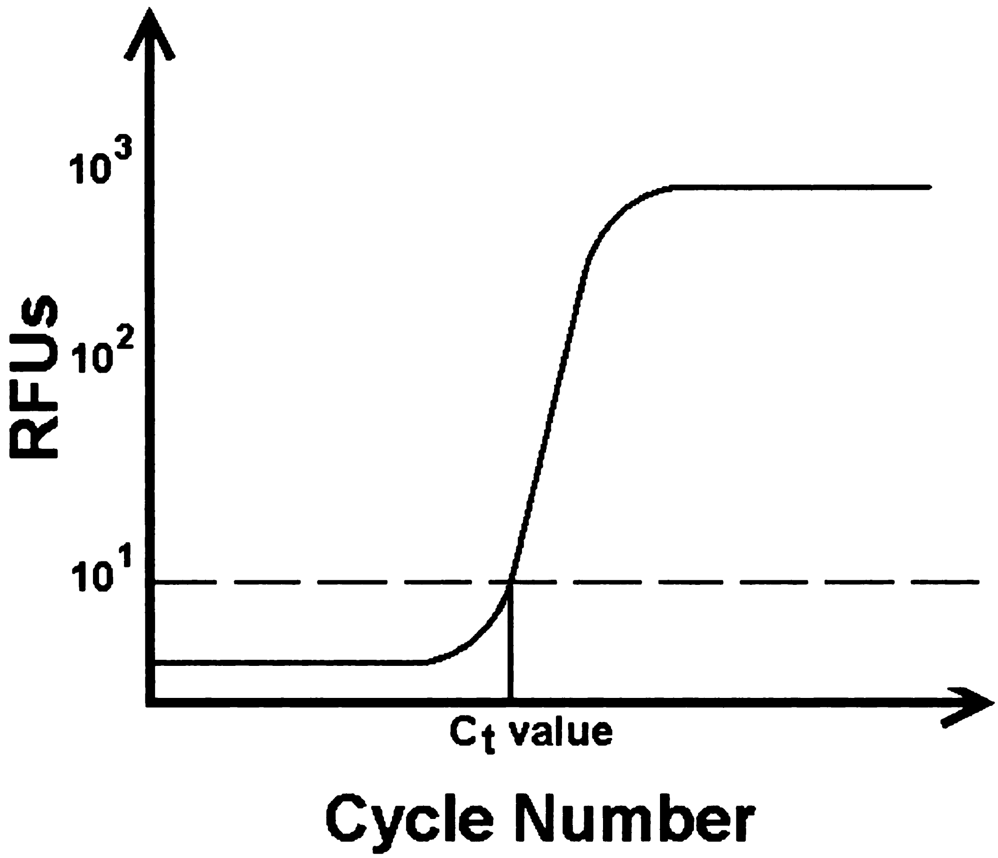

Figure 3: A Real-time PCR Amplification Curve
A typical amplification plot shows the number of PCR cycles plotted against relative fluorescent units (RFUs) values. As more DNA is amplified, the fluorescent signal increases, represented by the sigmoidal curve. When reaction components become limited, product accumulation stops and the fluorescent signal plateaus. The segmented line represents the threshold value. The cycle threshold (Ct) value illustrates the cycle where the amplification signal crosses the threshold.

SYBR® Green Real-Time PCR

SYBR® Green is an intercalating dye that fluoresces when bound to double stranded DNA. As demonstrated in Figure 4, when two complementary strands of DNA anneal, the SYBR® Green dye binds to the DNA and a fluorescent signal is emitted. Therefore, as more double stranded DNA is synthesized during PCR, more fluorescence is emitted.

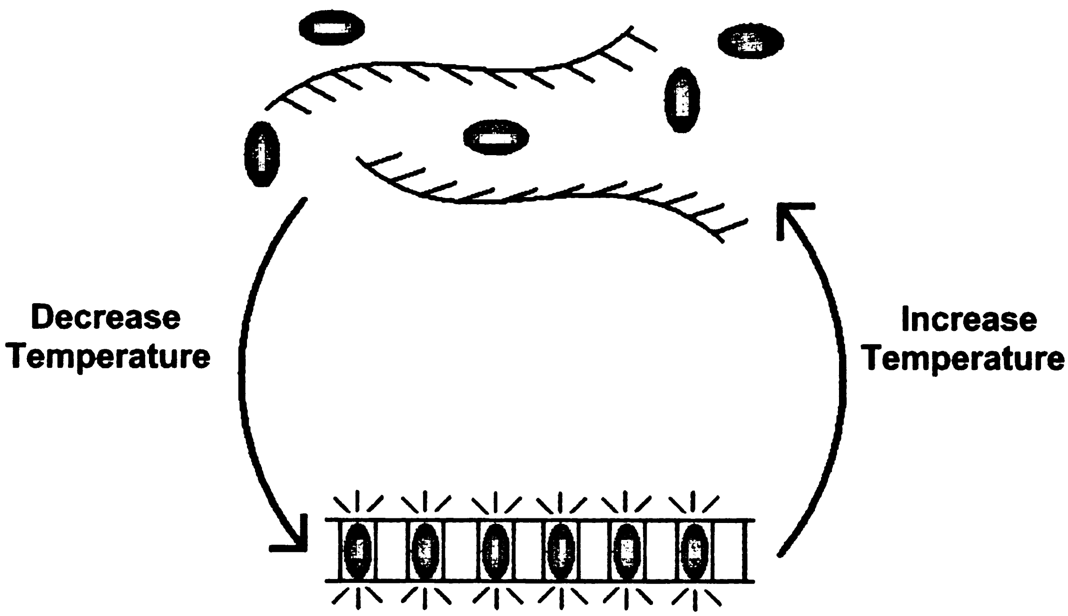

Figure 4: SYBR® Green Dye Properties
The ovals represent the SYBR® Green dye. As double stranded DNA is synthesized during PCR, more dye binds, thereby causing an increase in fluorescence. Conversely, when the reaction temperature increases and the double stranded DNA denatures to become single stranded, the SYBR® Green dye does not bind and no fluorescence is emitted.

One disadvantage with SYBR® Green rtPCR is that dye binding is non-specific. Therefore, if any non-target DNA is present, it too will generate a fluorescent signal (Foy and Parkes, 2001). To distinguish desired amplicons from non-target DNA, a dissociation reaction is run post-amplification, in which the temperature of the solution is slowly increased (Figure 5). At a temperature specific for the amplicon, the DNA dissociates, causing the SYBR® Green dye to fall away, decreasing the fluorescent signal. The real-time detection system monitors this change in fluorescence and creates a unique dissociation curve that can differentiate products within the reaction (Foy and Parkes, 2001).

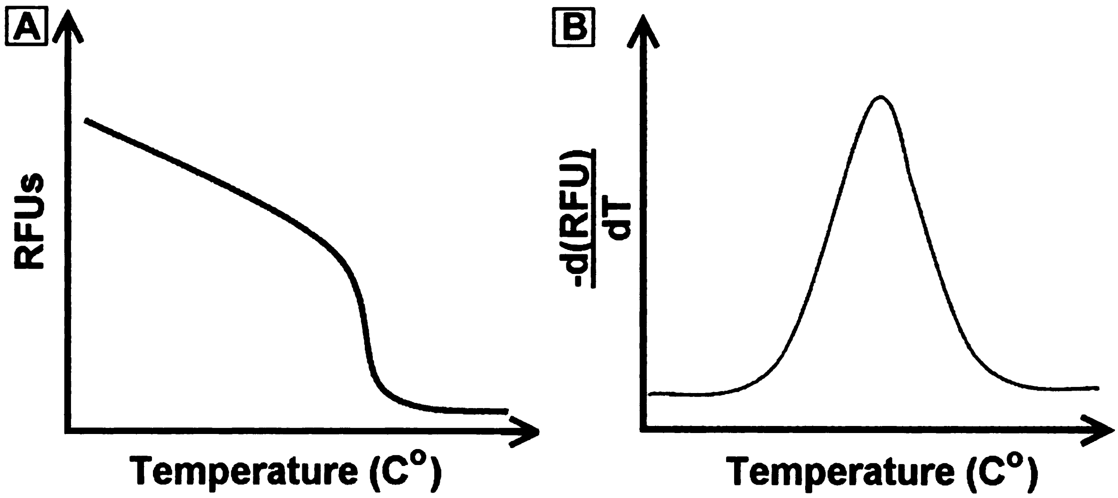

Figure 5: SYBR® Green Dissociation Curve
(A) An example of a standard dissociation curve performed after SYBR® Green real-time PCR. With a slow increase in temperature, strand dissociation occurs, causing the SYBR® Green dye to fall away, leading to a drop in fluorescence. Amplicons dissociate at specific temperatures creating a characteristic dissociation curve for a desired products within the reaction. The dissociation curve is displayed on a plot of RFU verses temperature (C°). (B) When monitoring fluorescence, the real-time detection system also plots the change in fluorescence over time (d(RFU)/dT) against an increase in temperature. This creates a peak at a DNA product's specific dissociation temperature.

TaqMan® PCR

Unlike SYBR® Green rtPCR, TaqMan® rtPCR technology uses fluorescent probes to monitor the amplification of a specific DNA sequence. The probe is a short sequence of DNA that is complementary to an internal region of an amplicon, attached to either end of the probe are a reporter dye and a non-fluorescent quencher (Figure 6). When the two are in close proximity, the fluorescence of the dye is quenched, and no signal is seen by the camera. During the PCR annealing step, the probe binds to the target sequence, allowing the DNA polymerase to cleave the dye from the probe as it builds the new strand of DNA. This separates the quencher from the reporter dye, allowing it to emit a fluorescent signal. The more target DNA that exists, the more probes are cleaved and fluorescent signal produced (Foy and Parkes, 2001).

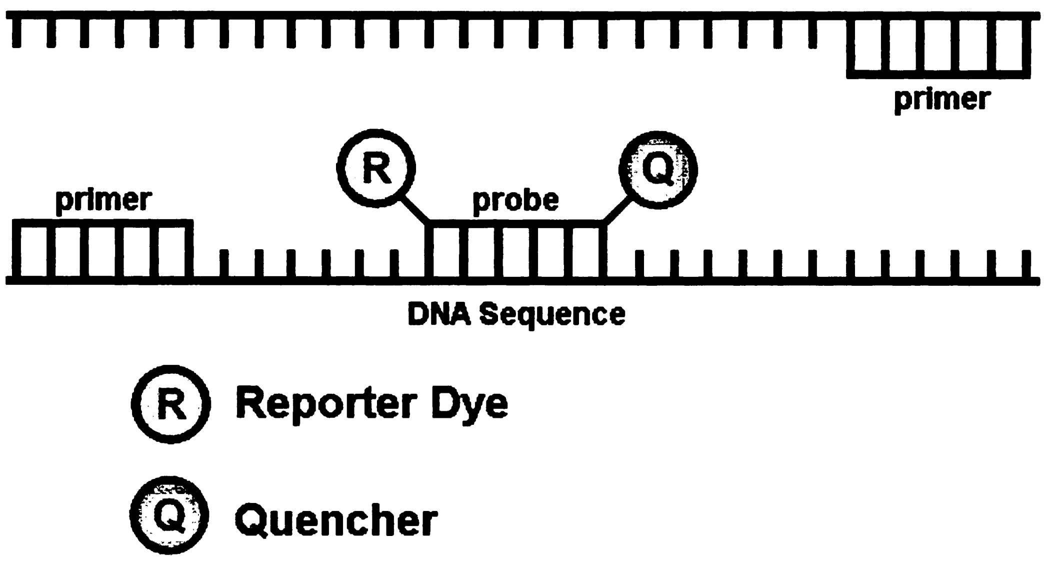

Figure 6: TaqMan® Real-time PCR Probe
A TaqMan® probe has a reporter dye on one end and a quencher on the other end. When the two are in close proximity, the fluorescence of the dye is quenched. After the probe anneals to the target sequence, polymerase begins to extend the primers. The reporter dye is then cleaved from the probe, resulting in increased florescence.

Research Goal

The object of the research presented here was to develop a sexing technique that is more sensitive than the current sexing methods for use on low quality DNA, as seen with forensic evidence. The standard molecular sexing technique used in forensic laboratories was represented by amplifying the amelogenin gene using SYBR® Green rtPCR. In contrast, the DYZ1 and Alu repetitive elements, being unrelated to one another, could be typed simultaneously (multiplexed), and were analyzed using TaqMan® technology. Analysis of high molecular weight (HMW) and artificially degraded DNA, along with low quality tissue DNA, were performed using the amelogenin and the DYZ1/Alu assay and the sensitivity and accuracy of the methods compared.

The Michigan State University (MSU) Forensic Biology Laboratory regularly works with sub-optimal DNA samples. For example, Graffy and Foran (2005) obtained hair from 30 individuals, removed the roots, and isolated hair shaft DNA using two techniques: a standard glass grinding/organic extraction and a novel alkaline digestion they developed. Nuclear DNA is notoriously difficult to obtain from hair shafts; therefore its testing is largely ignored. Since these hair shafts were expected to contain low quality nuclear DNA and the sex of the hair donors was known, they were ideal for analysis with the sex determining assays. The DNA from the hair shafts was sexed in a blind study with the amelogenin and DYZ1/Alu assays to compare the accuracy of each sexing technique.

The Forensic Biology Laboratory also analyzes DNA extracted from human skeletal remains, which may be fresh or quite ancient. Once again, it is difficult or often impossible to obtain nuclear DNA results from ancient skeletal material. The bones used in this study were collected from two ancient Albanian burial sites, the Triconch Palace and Merchant's House in the ancient city of Butrint, and a large tumulus (burial mound) located in Kamenica. The Triconch Palace and Merchant's House, a complex of buildings near the Butrint city wall on the bank of the Vivari Channel, date to 5th – 7th century A.D. and 13th – 15th century A.D., respectively. Hodges et al. (2000) described the Triconch Palace as originally a single family dwelling that later became a semi-public building. During the excavations of the Palace, numerous skeletal remains were unearthed within the rooms of the structure. A map of the burials in the Triconch Palace and Merchant's House is displayed in Figure 7. Multiple burial clusters are located in the palace, with an additional cluster in the southwest corner of the Merchant's House. Rauzi (2007) extracted DNA from several of these remains and analyzed the mitochondrial sequences to examine the maternal relatedness of the individuals within each cluster.

Figure 7: Map of the Triconch Palace and Merchant's House
Burial locations are displayed along with the palace rooms and the Merchant's House in the southwest corner. Letters distinguish the rooms of the palace. Burials are labeled with a four-digit number and depicted as a bold line ending with a dot showing the location of the head among the remains.

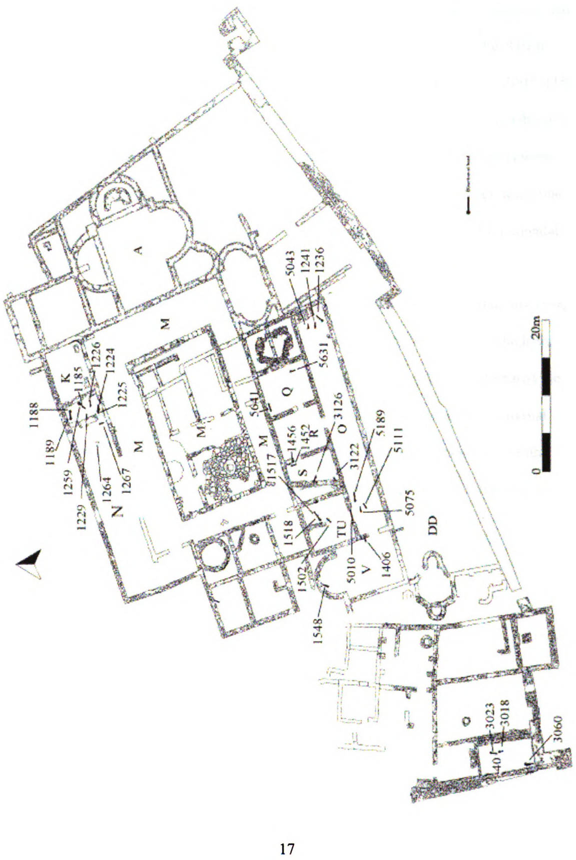
A
M
K
1188
1185
1226
1224
1225
1189
1259
1264
1267
1229
N
M
5043
1241
1236
5631
Q
5641
3126
O
R
1456
1452
M
S
1517
3122
5189
5111
5075
DD
1518
TU
1502
5010
V
1406
1548
3023
3018
3060
40
0
20m

The tumulus in Kamenica is the largest tumulus in Albania, with a diameter of 40 m, containing approximately 800 burials. As depicted in the burial maps in Figures 8 and 9, the original structure of the tumulus consisted of a double ring of rocks, the "Great Circle" 15 m in diameter, containing 35 burials covered in soil, and dating to 1200 – 1150 BC. Two hundred additional burials were placed on top of the central circle, and dated to 1150 – 650 BC. Around 650 BC, the burial pattern changed in which individuals were covered with rocks instead of buried under soil. These were encircled by rock walls that interconnected to make large formations called "Monumental Structures." Monumental Structure 1.1 and 3 are illustrated on the maps in Figures 8 and 9.

Most of the inhumations at Kamenica consisted of only one individual; however, there were numerous "double burials" or two individuals per grave, some of which are labeled with stars in Figures 8 and 9 (Bejko et al. 2006). Clemmer (2003) compared the mitochondrial DNA of several of the double burial remains to examine their maternal relatedness. In addition, Rennick (2005) extracted DNA from several remains within Monumental Structure 3 and analyzed mitochondrial DNA to determine if the structure might be a family grave site, or was a mixture of unrelated individuals.

Figure 8: Bottom Layer of the Kamenica Tumulus
The map depicts the lower (oldest) layer of the tumulus (1200 – 650 BC). The double ring of rocks is displayed in the upper left corner. Monumental Structure 1.1 is located in the upper right corner and Monumental Structure 3 is in the lower left corner of the map. Stars indicate double burials within the tumulus tested by Clemmer (2005).

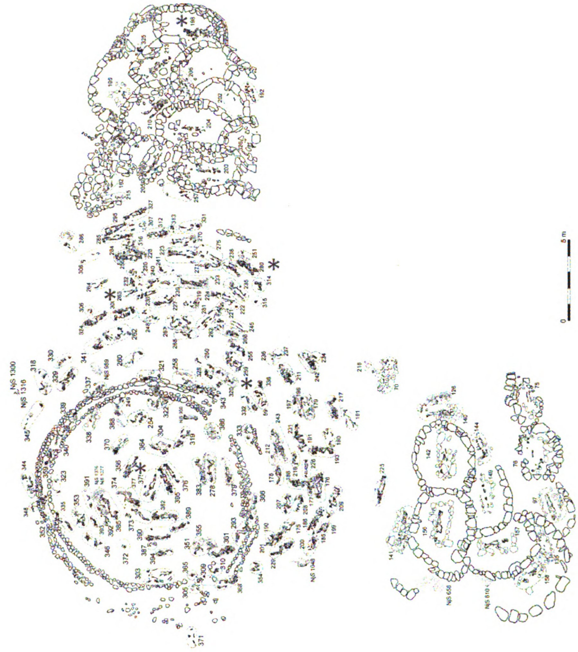

Figure 9: Top Layer of the Kamenica Tumulus
The map depicts the upper layer of the tumulus (1150 – 650 BC). The double ring of rocks is displayed in the upper left corner. Monumental Structure 1.1 is located in the upper right corner and Monumental Structure 3 is in the lower left corner of the map. Stars indicate double burials within the tumulus tested by Clemmer (2005).

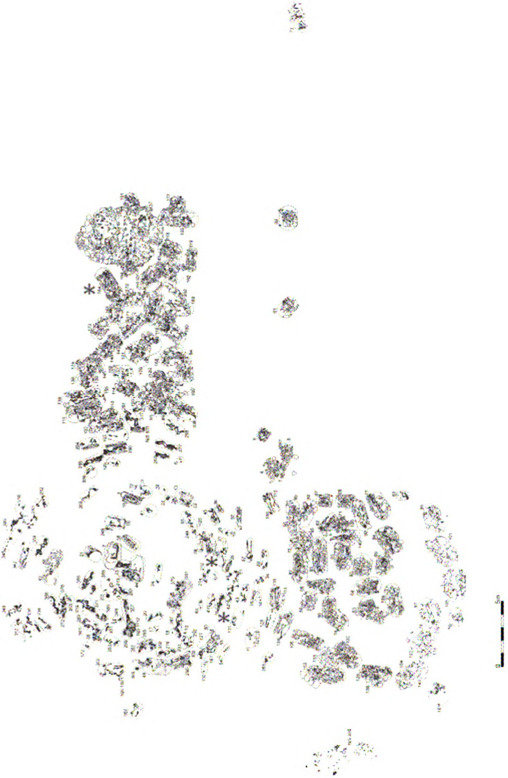

The hair shafts and skeletal remains provide a good representation of the condition of some evidence submitted to a forensic laboratory for DNA analysis. Unfortunately, because of the sub-optimal nature of the DNA, such samples are often overlooked for DNA analysis. If these samples were analyzed with the standard molecular sexing techniques, sex determination would be inconsistent and unreliable. The DYZ1/Alu assay, however, yields a sexing result for these low quality samples, providing valuable information for a forensic investigation.

MATERIALS AND METHODS

Control DNA

Single source male DNA (20 ng/µL), developed in the MSU Forensic Biology Laboratory, was used as the male control. K562 High Molecular Weight DNA (Promega) at a stock concentration of 10 ng/µL was used as a female control.

DNase Digestion

DNase I was used to digest 3.15 µg of single source male DNA, simulating degraded DNA. The reaction was performed on ice and included 3 U of Roche's recombinant RNase free DNase I, 5 µL of 10x incubation buffer, and sterile water (Fisher) to a final reaction volume of 50 µL. Fifteen microliter aliquots were removed at time intervals of 0, 30, and 60 seconds and placed in 5 µL of 20 mM EDTA. Aliquots were immediately placed in a 95°C water bath for 5 minutes to stop digestion. DNA from each time aliquot was separated on a 2% gel to estimate the level of digestion.

HMW DNA and digested DNA were serially diluted 15-fold and molecularly sexed in duplicate. HMW DNA ranged from 20 ng to 1.76 fg, while the digested DNA ranged from 47 ng to 4.13 fg.

Hair Shaft DNA

Volunteers' hair shafts, along with questionnaires regarding sex, population ancestry, hair color, and hair treatments (Table 1), had been previously collected (Graffy and Foran, 2005). DNA was extracted from the hair shafts by one of two methods: a glass grinding/organic extraction or an alkaline digestion. In the current research, the hair shaft DNA was analyzed blind for sex determination.

Table 1: Analyzed Hair Samples
The sex and population ancestry is recorded, along with any hair treatments performed. (Graffy, 2003). Hair without treatment is denoted by (---).

Hair Identifier	Declared Sex	Population Ancestry	Hair Treatment
8	Female	African	perm/relaxer within year
9	Female	Caucasian	dye within year
10	Female	Caucasian	blow dry
11	Male	Caucasian	---
12	Female	Caucasian	blow dry
13	Female	Hispanic	blow dry/dye within month
14	Female	Caucasian	dye within month
16	Female	Asian	blow dry/dye within year
17	Male	Caucasian	---
19	Female	Caucasian	dye within month
20	Female	Asian	blow dry
22	Male	Caucasian	---
23	Female	African	blow dry /perm/relaxer within year
24	Male	Caucasian	blow dry
27	Male	Asian	blow dry
28	Female	Caucasian	blow dry/ dye within year
29	Male	Caucasian	---
32	Female	Caucasian	---
35	Female	Caucasian	blow dry/ dye/perm/relaxer within
36	Female	Caucasian	blow dry/ dye within month
37	Female	Caucasian	blow dry/ dye within month
38	Female	Hispanic	blow dry/ dye within year
43	Female	Asian	blow dry/ dye within month
46	Male	Caucasian	---
54	Female	African	blow dry
55	Male	African	---
56	Female	African	perm/relaxer within month
57	Female	Asian	---
59	Female	Asian	---
60	Female	African	dye/perm/relaxer within month

Ancient Skeletal DNA

DNA was extracted from skeletal samples excavated from two Albanian archeological sites: the Triconch Palace (5^{th} – 7^{th} century AD) and Merchant's House (13^{th} – 15^{th} century AD) in Burtrint, Albania (Rauzi, 2007), and Monumental Structure 3 within the tumulus in Kamenica, Albania (7^{th} – 6^{th} century BC) (Rennick, 2005). Table 2 displays the specific bones from which DNA was extracted, the century the remains were buried, and the anthropological age and sex estimation for each individual.

Table 2: Analyzed Skeletal Samples
An identifier was given to each bone corresponding to the respective burial site. The specific bones are listed, along with the estimated age of each individual, the century the remains were buried, and the anthropological age and sex estimates for each burial. Partial or juvenile bones that were unable to be sexed by anthropological methods are listed as unknown. Remains from Burtrint, Albania are labeled BA and remains from Kamenica, Albania are labeled KA. (Rauzi, 2007; Rennick, 2005).

Bone Identifier	Specific Bone	Century	Age	Anthropological Sex
BA Bone				
1185.1	fibula shaft	5^{th} – 7^{th} A.D.	Adult	Unknown
1187.1	right radius	5^{th} – 7^{th} A.D.	30 – 45	Male
1187.2	right fibula	5^{th} – 7^{th} A.D.	30 – 45	Male
1188.1	left humerus shaft	5^{th} – 7^{th} A.D.	11 – 13	Unknown
1188.2	right petrous	5^{th} – 7^{th} A.D.	11 – 13	Unknown
1224.1	left petrous	5^{th} – 7^{th} A.D.	3 – 4 yrs	Unknown
1224.2	right humerus	5^{th} – 7^{th} A.D.	3 – 4 yrs	Unknown
1225.1	right petrous	5^{th} – 7^{th} A.D.	3 – 4 yrs	Unknown
1226.1	right fibula	5^{th} – 7^{th} A.D.	35 – 45	Male
1226.2	left ulna midshaft	5^{th} – 7^{th} A.D.	35 – 45	Male
1229.2	humeral shaft	5^{th} – 7^{th} A.D.	3 – 6 mos	Unknown
1236.1	fibula midshaft	5^{th} – 7^{th} A.D.	23 – 27	Female
1236.2	left ulna midshaft	5^{th} – 7^{th} A.D.	23 – 27	Female
1259.1	left femur	5^{th} – 7^{th} A.D.	10 – 12	Unknown
1264.1	tibia cortical fragment fr. Distal	5^{th} – 7^{th} A.D.	6 – 8 yrs	Unknown
1264.2	fibula midshaft	5^{th} – 7^{th} A.D.	6 – 8 yrs	Unknown

Table 2 (cont'd)

Bone Identifier	Specific Bone	Century	Age	Anthropological Sex
BA Bone				
1518.1	humeral cortical	$5^{th} - 7^{th}$ A.D.	40+ yrs	Male
1518.2	fibula midshaft	$5^{th} - 7^{th}$ A.D.	40+ yrs	Male
5010.1	fibula midshaft	$5^{th} - 7^{th}$ A.D.	35 – 45	Female
5010.2	humerus midshaft	$5^{th} - 7^{th}$ A.D.	35 – 45	Female
3023.1	petrous portion	$13^{th} - 15^{th}$	25 – 35	Male
KA Bone				
66	humerus	$7^{th} - 6^{th}$ B.C.	n/a	Male
66	femur	$7^{th} - 6^{th}$ B.C.	n/a	Male
75	tibia	6^{th} B.C.	45+ yrs	Male
75	femur	6^{th} B.C.	45+ yrs	Male
75	petrous portion	6^{th} B.C.	45+ yrs	Male
82	radius	$7^{th} - 6^{th}$ B.C.	old	Male
82	petrous portion	$7^{th} - 6^{th}$ B.C.	old	Male
85	femur	$7^{th} - 6^{th}$ B.C.	22 – 28	Male
97	tibia	$7^{th} - 6^{th}$ B.C.	n/a	Male
97	femur	$7^{th} - 6^{th}$ B.C.	n/a	Male
102	humerus	$7^{th} - 6^{th}$ B.C.	middle	Female
102	petrous portion	$7^{th} - 6^{th}$ B.C.	middle	Female
104	humerus	$7^{th} - 6^{th}$ B.C.	22 – 28	Male
104	femur	$7^{th} - 6^{th}$ B.C.	22 – 28	Male
142	pelvis	7^{th} B.C.	45+ yrs	Male
142	petrous portion	7^{th} B.C.	45+ yrs	Male
142	humerus	7^{th} B.C.	45+ yrs	Male
156	femur	7^{th} B.C.	29 – 35	Male
156	petrous portion	7^{th} B.C.	29 – 35	Male
156	humerus	7^{th} B.C.	29 – 35	Male

Each bone was drilled using a Dremel rotary tool (Dremel) and the resultant powder was digested with proteinase K and digestion buffer. DNA was extracted using a standard organic extraction and purified using Microcon-YM30 (Millipore) column filters (Rauzi, 2007; Rennick, 2005).

Amelogenin Assay

AMEL-X and AMEL-Y Primer Optimization

The forward primers for the amelogenin assay (Table 3) were designed using Primer3 software (Rozen and Skaletsky, 2007). The AMEL-X forward primer spanned the 6 bp deletion on the amelogenin gene on the X-chromosome, while the AMEL-Y forward primer spanned the homologous sequence on the Y-chromosome (Figure 10). The British reverse (BR) primer (Sullivan et al. 1993) was used with both forward primers. The AMEL-X/BR and the AMEL-Y/BR primer sets resulted in 69 bp and 77 bp products respectively.

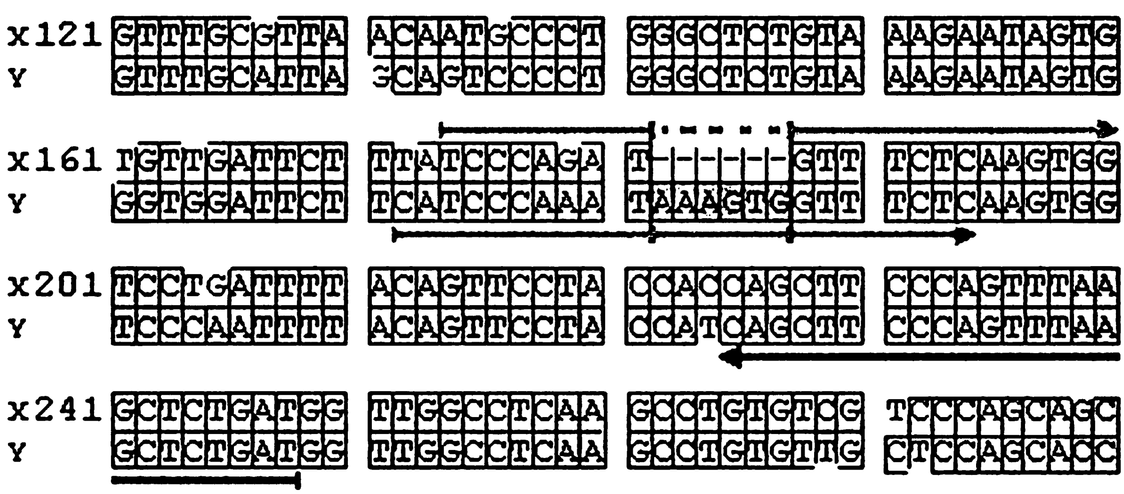

Figure 10: Amelogenin Sequences and Primer Location
A portion of the amelogenin sequence on the X and Y chromosome is displayed on the top and bottom rows, respectively. The gray boxes show the 6 bp deleted from the X chromosome. The lighter arrows denote the position of the X and Y forward primers, while the darker arrow indicates the British reverse primer. The X chromosome primer set resulted in a 69 bp product and the Y chromosome product was 77 bp. (Modified from Sullivan et al. 1993).

The optimal annealing/extension temperature was determined using 15 µL reactions including 1x Fast SYBR® Green Master Mix (Roche), 2 µM AMEL-X or AMEL-Y, 2 µM BR, 1 ng male or female DNA, and sterile water (Fisher). Cycling parameters were a 95°C hold for 10 min and 40 cycles of a 95°C denaturing step for 15 sec, and an annealing/extension gradient from 50°C to 60°C for 1 min. Dissociation parameters were a 95°C hold for 1 min, a 55°C hold for 1 min, and a dissociation range from 55°C to 95°C. PCR reactions were performed on an iQ™5 Multicolor Real-Time Detection System and iCycler (Bio-Rad), and analyzed with Bio-Rad iQ5 – Standard Edition software. The products were separated on a 4% agarose gel to determine if amplicons were the expected size. The annealing/extension temperature that yielded an amplification curve that crossed the threshold and a peak on the dissociation curve at the appropriate temperature were considered optimal. Optimization of AMEL-X, AMEL-Y, and BR primer concentrations was performed at 200 nM, 1 µM, and 2 µM. Cycling and dissociation parameters outlined above were used with the optimized annealing/extension temperature. The primer concentrations that yielded an amplification curve that crossed the threshold and a peak on the dissociation curve at the appropriate temperature were considered optimal.

Table 3: Amelogenin Primer Sequences
Primer names and sequences are given. AMEL-X and AMEL-Y are the forward primers targeting the 6 bp deletion region on the X and Y chromosome respectively. BR is the British reverse primer used with both forward primers.

Primer Identifier	Primer Sequence
AMEL-X	5'-TCCCAGATGTTTCTCAAGTGG-3'
AMEL-Y	5'-CATCCCAAATAAAGTGGTTTCTC-3'
BR	5'-ATCAGAGCTTAAACTGGGAAGCTG-3'

Amelogenin Assay Parameters

The amelogenin assay included 15 µL reactions with either 1x Fast SYBR® Green Master Mix (Roche) or 1x Power SYBR® Green Master Mix (Applied Biosystems), 1 µM AMEL-X or AMEL-Y primers, 2 µM BR primer, 1 µL DNA, and sterile water (Fisher). Reactions with samples subject to inhibition, such as hair or bone, contained 10 µg BSA. Cycling and dissociation parameters were the same as those optimized for the amelogenin primers. Amelogenin assays were run in triplicate.

DYZ1/Alu Assay

Alu Primer and Probe Optimization

Alu primer and probe sequences (Table 4) were designed by Nicklas and Buel (2005), yielding a product size of 127 bp targeted as a positive human control. The TaqMan® Alu probe was labeled with Hex reporter dye on the 5' end and the non fluorescent quencher DBH1 on the 3'end. Alu forward (Alu-F) and reverse (Alu-R) primers were optimized at 200 nM, 500 nM, and 900 nM, using 1x Fast SYBR® Green Master Mix (Roche), 1 ng male DNA, and sterile water (Fisher) to 15 µL. Cycling parameters were a 95°C hold for 10 min, then 50 cycles of a 95°C denaturing step for 15 sec and 60°C annealing/extension step for 1 min. The dissociation parameters were a 95°C hold for 1 min, a 55°C hold for 1 min, and a melt range from 55°C to 95°C and were performed to determine if the amplicon dissociated at the expected temperature. Products were separated on a 4% agarose gel to determine if the amplicon was the expected size. The primer concentrations and annealing/extension temperature that yielded an amplification curve that crossed the threshold and a peak on the dissociation curve at the appropriate temperature were considered optimal. An optimization annealing temperature gradient assay, from 55°C to 63°C, was then performed. Optimized conditions were used for subsequent experiments.

Alu probe concentration was optimized at 50 nM, 150 nM, and 250 nM. Male and female DNA at 100 pg and a 1:15 dilution were used in 15 µL reactions including 1x iQ Supermix (Bio-Rad), 500 nM Alu-F, 900 nM Alu-R, the respective Alu probe concentrations, and sterile water (Fisher), and cycling parameters outlined above. The probe concentration that yielded an amplification curve that crossed the threshold for both male and female DNA was deemed optimal.

DYZ1 Primers and Probe Optimization

The primer pair and probe targeting the DYZ1 locus with an expected product size of 143 bp were designed by William Kiffmeyer, Applied Biosystems Field Applications Specialist (Jackson, 2005) (Table 4). The DYZ1 probe was labeled with 6-FAM reporter dye on the 5' end along with a minor groove binding (MGB) non-fluorescent quencher on the 3' end. DYZ1 primer optimization was performed using concentrations of 200 nM, 500 nM, and 900 nM and the same cycling were used for Alu primer optimization. An annealing temperature gradient assay, from 55°C to 63°C, was also performed for primer optimization. The dissociation parameters were the same as Alu primer optimization and were performed to determine if the amplicon dissociated at the expected temperature. Fifteen microliter reactions included 1x iQ™ SYBR® Green Supermix (Bio-Rad), respective concentrations of DYZ1 forward (DYZ1-F) and reverse (DYZ1-R) primers, 1 ng male DNA, and sterile water (Fisher). Products were separated on a 4% agarose gel to determine if the amplicon was the expected size. The primer concentrations and annealing/extension temperature that yielded an amplification curve that crossed the threshold and a peak on the dissociation curve at the expected temperature were considered optimal.

The DYZ1 probe concentration was optimized at 50 nM, 150 nM, and 250 nM using the same cycling parameters as primer optimization above. Male and female DNA at 100 pg and a 1:15 dilution were used in 15 µL reactions containing 1x iQ Supermix (Bio-Rad), 500 nM DYZ1-F, 500 nM DYZ1-R, the respective DYZ1 probe concentrations, and sterile water (Fisher). The probe concentration that yielded an amplification curve that crossed the threshold at the lowest Ct value for both male and female DNA was deemed optimal.

Table 4: Alu and DYZ1 Primer/Probe Sequences
Primer and probe names and sequences are given. DHEX and 6FAM are fluorescent dyes on the 5' end of the Alu and DYZ1 probe, respectively. DBH1 is the non-fluorescent quencher on the 3' end of the Alu probe, while MGBNFQ is the minor groove binder non-fluorescent quencher on the 3' end of the DYZ1 probe.

Primer Identifier	**Primer Sequence**
Alu-F	5'-GAGATCGAGACCATCCCGGCTAAA-3'
Alu-R	5'-CTCAGCCTCCCAAGTAGCTG-3'
DYZ1-F	5'-GGCCTGTCCATTACACTACATTCC-3'
DYZ1-R	5'-GAATTGAATGGAATGGGAACGA-3'
Probe Identifier	**Probe Sequence**
Alu-Probe	5'-DHEX-GGGCGTAGTGGCGGG-DBH1-3'
DYZ1-Probe	5'-6FAM-ATTCCAATCCATTCCTTT-MGBNFQ-3'

DYZ1/Alu Assay

Primers and probes for the Alu and DYZ1 loci were then multiplexed in a TaqMan® rtPCR assay. Fifteen microliter reactions included 1x iQ Supermix (Bio-Rad), 500 nM Alu-F and DYZ1-F, 900 nM Alu-R and DYZ1-R, 250 nM Alu and DYZ1 probes, 1 µL DNA, and sterile water (Fisher). Reactions with samples subject to inhibition, such as hair or bone, contained 10 µg BSA. Each sample was analyzed in triplicate using the optimized conditions detailed above.

Contamination Control

Pipetters, pipette tips, tubes, racks, and sterile water (Fisher) were placed in a Spectrolinker ™ XL-1500 UV Crosslinker (Spectronics Corporation). Reactions were prepared in a Clean Spot PCR/UV Work Station (COY Laboratory Products) and a surgical mask, sleeves and two pairs of gloves were worn during preparation. Sterile water (Fisher) was filtered through a Microcon YM-30 (Millipore) and ultraviolet (UV) irradiated for 10 min. Primers for the DYZ1/Alu multiplex and the amelogenin assay were diluted using the purified sterile water and filtered through a Microcon YM-30 (Millipore).

The DYZ1/Alu multiplex, the iQ Supermix, primers and probes were UV irradiated for 0 seconds, 30 seconds (2.73 J/cm^2), 1.0 min (5.45 J/cm^2), 1.5 min (8.18 J/cm^2), 2.0 min (10.90 J/cm^2), 2.5 min (13.63 J/cm^2), and 3.0 min (16.36 J/cm^2). Fifteen µL reactions included each UV treated master mixes, 10 µg BSA, and either 100 pg male DNA as a positive control or sterile water as a negative control. A UV treatment that yielded amplification of both loci for the positive control and no amplification for the negative control was used for subsequent multiplex reactions.

RESULTS

Optimal Sexing Assay Conditions

Amelogenin Assay

Optimal primer concentrations for the amelogenin assay were 1 μM for both AMEL-X and AMEL-Y and 2 μM for the BR primer. The optimal annealing/extension temperature for was 58.5°C. Using the Fast SYBR® Green Master Mix (Roche), the AMEL-X dissociation curve demonstrated a peak between 73.5°C and 74.5°C, while AMEL-Y had a peak between 73°C and 75°C. Both amelogenin products yielded dissociation peaks between 74.5°C and 75.5°C using the Power SYBR® Green Master Mix (Applied Biosystems).

AMEL-X and AMEL-Y signals crossed the threshold using similar Ct values for male control DNA (Figure 11A) and the dissociation curves demonstrated peaks at the correct temperatures (Figure 11B). Conversely, only the AMEL-X signal crossed the threshold using female DNA (Figure 12A) and the respective peak on the dissociation curve was present (Figure 12B).

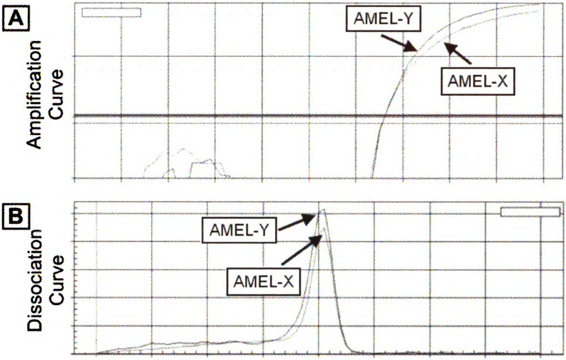

Figure 11: Amelogenin Amplification and Dissociation Curve for Male DNA
The AMEL-X and AMEL-Y target sequences from male control DNA were amplified. (A) The AMEL-X and AMEL-Y amplification plots (x-axis = cycle number, y-axis = RFU value, AMEL-X and AMEL-Y Ct value = 33 cycles). The bold line represents the threshold value of 10 RFUs. (B) Dissociation curves for the AMEL-X and AMEL-Y products (x-axis = temperature (°C), y-axis = -d(RFU)/dT, AMEL-X and AMEL-Y melt temperature = 75.5°C).

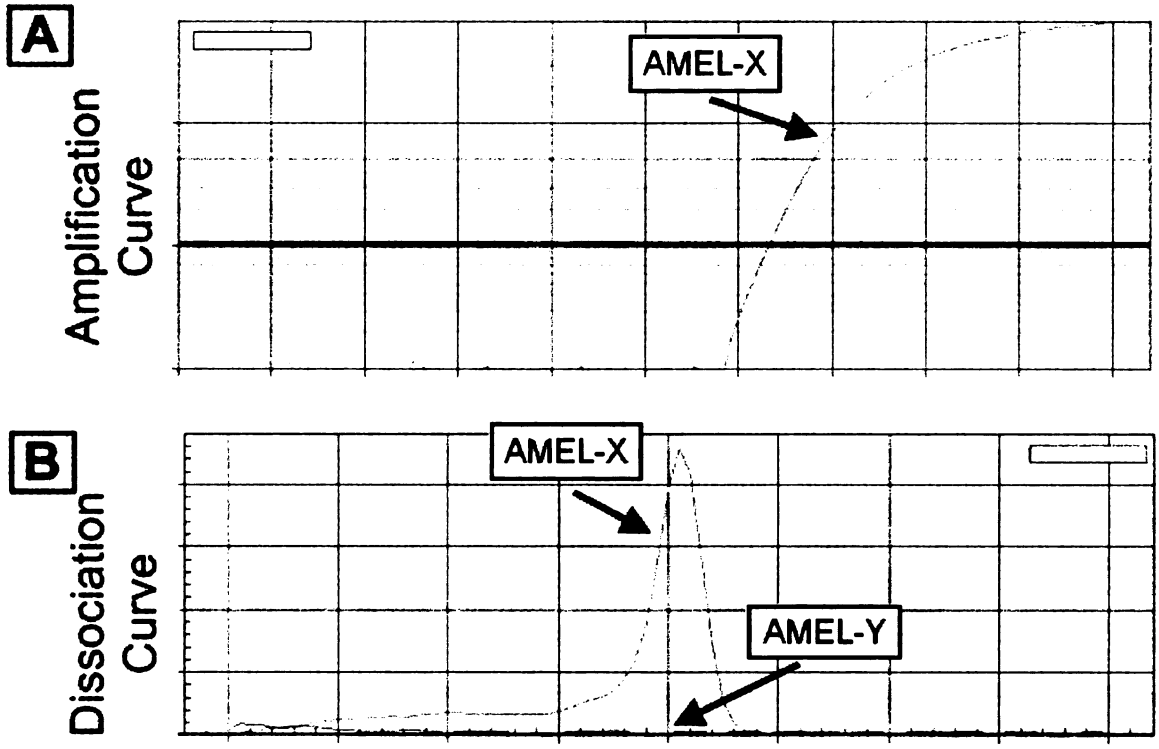

Figure 12: Amelogenin Amplification and Dissociation Curve for Female DNA
The AMEL-X target sequence from female control DNA was amplified. (A) The AMEL-X amplification plot (x-axis = cycle number, y-axis = RFU value, AMEL-X Ct value = 31 cycles). The bold line represents the threshold value of 10 RFUs. (B) The AMEL-X dissociation curve for female DNA, using no peak for the AMEL-Y product (x-axis = temperature (°C), y-axis = -d(RFU)/dT, AMEL-X melt temperature = 75.5°C).

DYZ1/Alu Assay

Optimal primer concentrations for DYZ1 were 500 nM for DYZ1-F and 900 nM for DYZ1-R, using a probe concentration of 250 nM. Optimal Alu primer concentrations were 500 nM for Alu-F and 900 nM for Alu-R, using a probe concentration of 250 nM. Optimized cycling parameters included a 95°C hold for 10 min, then 50 cycles of a 95°C denaturing step for 15 sec and 60°C annealing/extension step for 1 min. When the assay was run using control DNA, male DNA displayed an amplification curve crossing the threshold for both DYZ1 and Alu at similar Ct values (Figure 13A), while only the Alu signal crossed the threshold using female DNA (Figure 13B).

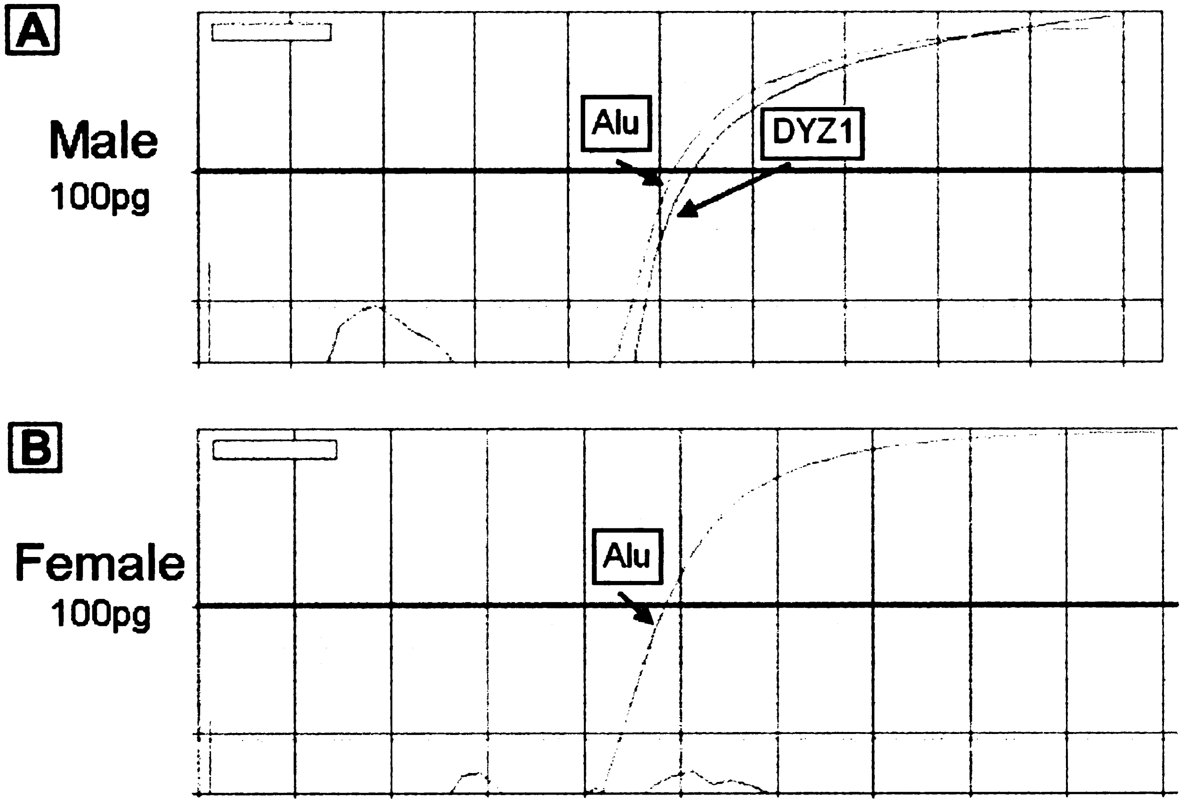

Figure 13: DYZ1/Alu Assay Amplification of Male and Female DNA
Amplification of 100 pg of male and female control DNA (x-axis = cycle number, y-axis = RFU value). The bold line represents the threshold value of 10 RFUs. (A) Male DNA displays a curve for both DYZ1 and Alu crossing the threshold at similar Ct values of 27 and 26 cycles, respectively, (B) while only Alu curve crossed the threshold at 24 cycles using female DNA.

DYZ1/Alu Assay UV Treatment

Negative controls produced a DYZ1 product during assay development, therefore the supermix and primers were UV irradiated. Probes were not UV irradiated so as not to cause interference using the fluorescent dyes. UV treatments of 30 seconds and 1 minute yielded DYZ1 product for the positive male control and no product for the negative control. Treatments of 1.5 minutes and higher produced no DYZ1 product for either the positive or negative control. Alu product was persistent using both negative and positive controls after all UV treatments, even at the longest irradiation of three minutes. Figure 14 represents a 4% agarose gel separating DYZ1 and Alu products for reactions UV irradiated for 30 seconds and non-UV treated reactions.

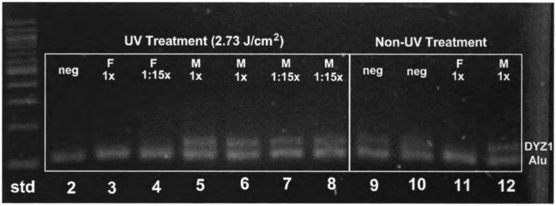

Figure 14: DYZ1/Alu Assay UV Treatment Agarose Gel
Four percent agarose gel showing amplification products of the DYZ1/Alu assay using UV treatment of 30 seconds (2.73 J/cm^2) (lanes 2 – 8) and non-UV treatment (lanes 9 – 12). (std = 100 bp size standard, neg = negative control, F = female DNA, M = male DNA, 1x = 100 pg HMW DNA, 1:15x = 15-fold dilution of 100 pg HMW DNA). The male control UV treatment was run in duplicate. The upper band represents the DYZ1 product and the lower band represents the Alu product. The UV treated reactions yielded a DYZ1 product using male DNA and no product using the negative and female DNA. The non-UV treated reactions yielded DYZ1 product from the negative and male DNA and no product for female DNA. Alu product was present in all reactions.

HMW and Digested DNA Dilution Series

The dilution series of HMW and digested male DNA demonstrated the sensitivity of the amelogenin and DYZ1/Alu assays. Table 5 shows that the amelogenin assay generated a positive result in at least one replicate containing as little as 88.9 pg of HMW DNA, while the DYZ1/Alu assay gave a positive result using as little as 0.0623 pg of HMW DNA. The dilution series of DNase digested male DNA demonstrated that the amelogenin assay generated a positive result in at least one replicate containing as little as 208.9 pg of digested DNA, while the DYZ1/Alu assay gave a positive result using as little as 0.00413 pg of digested DNA.

Table 5: Amplification Success of the High Molecular Weight DNA and DNase Digested Male DNA Dilution Series

Diluted DNAs that produced a correct result for each DNA concentration are shown for the amelogenin and DYZ1/Alu assays. The amelogenin assay detected both the AMEL-X and AMEL-Y loci in HMW DNA quantities as low as 88.89 pg, and 208.9 pg of digested DNA. HMW DNA was detected for both the Alu and DYZ1 loci down to 0.0623 pg, while digested DNA was detected down to 0.00413 pg.

Dilution Series	Amelogenin Assay		DYZ1/Alu Assay	
HMW DNA	**AMEL-X**	**AMEL-Y**	**Alu**	**DYZ1**
20000 pg	2	2	1	1
1330 pg	2	2	2	2
88.89 pg	2	1	2	1
5.93 pg	0	0	2	2
0.393 pg	0	0	2	2
0.0623 pg	0	0	2	1
0.00176 pg	0	0	2	0
Digested DNA	**AMEL-X**	**AMEL-Y**	**Alu**	**DYZ1**
47000 pg	2	2	2	2
3130 pg	2	2	2	2
208.9 pg	2	2	2	2
13.93 pg	0	2	2	2
0.928 pg	0	0	2	1
0.0619 pg	0	0	2	1
0.00413 pg	0	0	2	1

The AMEL-Y assay of 88.89 pg HMW DNA generated positive results for only one of two replicates, while 88.89 pg and 0.0623 pg of HMW DNA and 0.928 pg, 0.0619 pg, and 0.00413 pg of digested DNA produced positive results for the DYZ1 locus in one of two replicates. In addition, 20000 pg of HMW DNA produced a positive result in one out of two replicates of the DYZ1/Alu assay. Figure 15 demonstrates the amplification plot of both replicates for 20000 pg HMW DNA using the DYZ1/Alu assay. Replicate one produced a curve for the Alu product that did not cross the threshold and no curve for DYZ1. Replicate two produced a non-sigmoidal curve and a lower Ct value for the DYZ1 product than the Alu amplification curve (Figure 15).

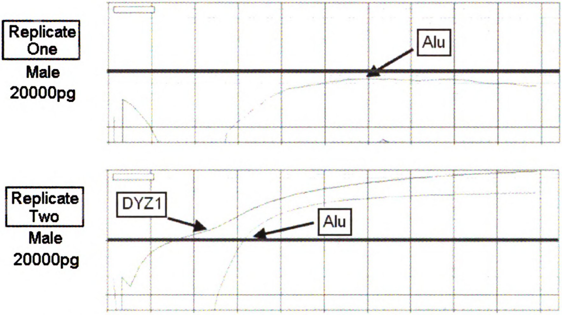

Figure 15: Amplification Plots of 20000 pg HMW DNA using the DYZ1/Alu Assay
The plot for replicate one displays a curve for the Alu product which does not cross the threshold, and no curve for DYZ1. The plot of replicate two displays a non-sigmoidal curve with a Ct value of 7 cycles for DYZ1and an Alu amplification curve that crossed threshold at a higher Ct value of 16 cycles (x-axis = cycle number, y-axis = RFU value). The bold line represents the threshold value of 10 RFUs.

Sexing of Hair Shaft DNA

Sex determination for 30 hairs using the amelogenin assay and the DYZ1/Alu assay, and the known sex for each hair donor, are displayed in Table 6.

Table 6: Sexing Results of Hair Shaft DNA

Sex determined using the amelogenin and DYZ1/Alu assays are compared to the known sex of each hair donor. (*) represent sexing results that do not match the known sex. An inconclusive result was given to hairs when a sex result could not be determined. The organic DNA extractions for each hair were sexed and hairs with incorrect sexing results were reanalyzed using the alkaline digestion, denoted by (†).

Hair Donor Identifier	Amelogenin Assay	DYZ1/Alu Assay	Known Sex
8	female	female	female
9	female	female	female
10	inconclusive	female	female
11	male	male	male
12	inconclusive	female	female
13	female	female	female
14	female	female	female
16	male*	female	female
17	female*	male	male
19	female	male*†	female
20	female	female	female
22	inconclusive	male	male
23	inconclusive	female	female
24	inconclusive	male	male
27	inconclusive	male	male
28	inconclusive	male*†	female
29	inconclusive	male	male
32	female	female	female
35	inconclusive	female†	female
36	female	female	female
37	female	female	female
38	male*	female	female
43	female	female	female
46	male	male	male
54	female	female	female
55	female*	male	male
56	female	female†	female
57	female	female	female
59	inconclusive	female	female
60	female	female	female

Amelogenin Assay

The amelogenin assay correctly sexed 16 hairs (53%), 14 females and 2 males. Additionally, ten hairs (33%) produced inconclusive results, as exemplified in Figure 16. The AMEL-X and AMEL-Y amplification curves crossed the threshold, but the peaks on the dissociation curve were lower than the correct temperature for sex determination.

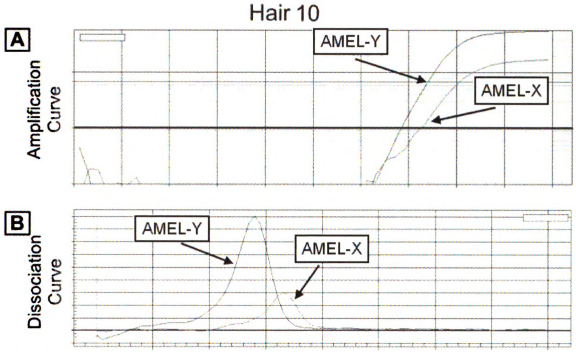

Figure 16: Inconclusive Sexing Result of Hair using the Amelogenin Assay
A female hair that yielded no sexing result. (A) The AMEL-X and AMEL-Y amplification plots (x-axis = cycle number, y-axis = RFU value). Both amplification curves crossed the threshold of 10 RFUs (bold line). The AMEL-X Ct value was 36 cycles and the AMEL-Y Ct value was 34 cycles. (B) The AMEL-X and AMEL-Y peaks on the dissociation curve (x-axis = temperature (°C), y-axis = -d(RFU)/dT, AMEL-X melt temperature = 72°C, AMEL-Y melt temperature = 69°C). The peaks for both products lower than the correct temperatures for sex determination.

Hairs 16 and 38 were incorrectly sexed as male using the amelogenin assay. An amplification and dissociation curves for one replicate from both are illustrated in Figures 17 and 18, respectively. For each, the AMEL-X and AMEL-Y amplification curves crossed the threshold and displayed a dissociation curve at the correct temperatures.

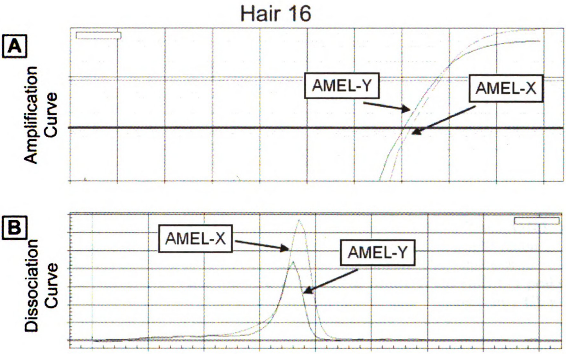

Figure 17: Female Hair 16 Sexing Result using the Amelogenin Assay
Hair 16 typed as male when the known sex was female. (A) The AMEL-X and AMEL-Y amplification plots (x-axis = cycle number, y-axis = RFU value). Both amplification curves crossed the threshold of 10 RFUs (bold line). The AMEL-X Ct value was 37 cycles and the AMEL-Y Ct value was 35 cycles. (B) The AMEL-X and AMEL-Y peaks on the dissociation curve were at the correct temperatures (x-axis = temperature (°C), y-axis = -d(RFU)/dT, AMEL-X melt temperature =73.5°C, AMEL-Y melt temperature = 73°C.).

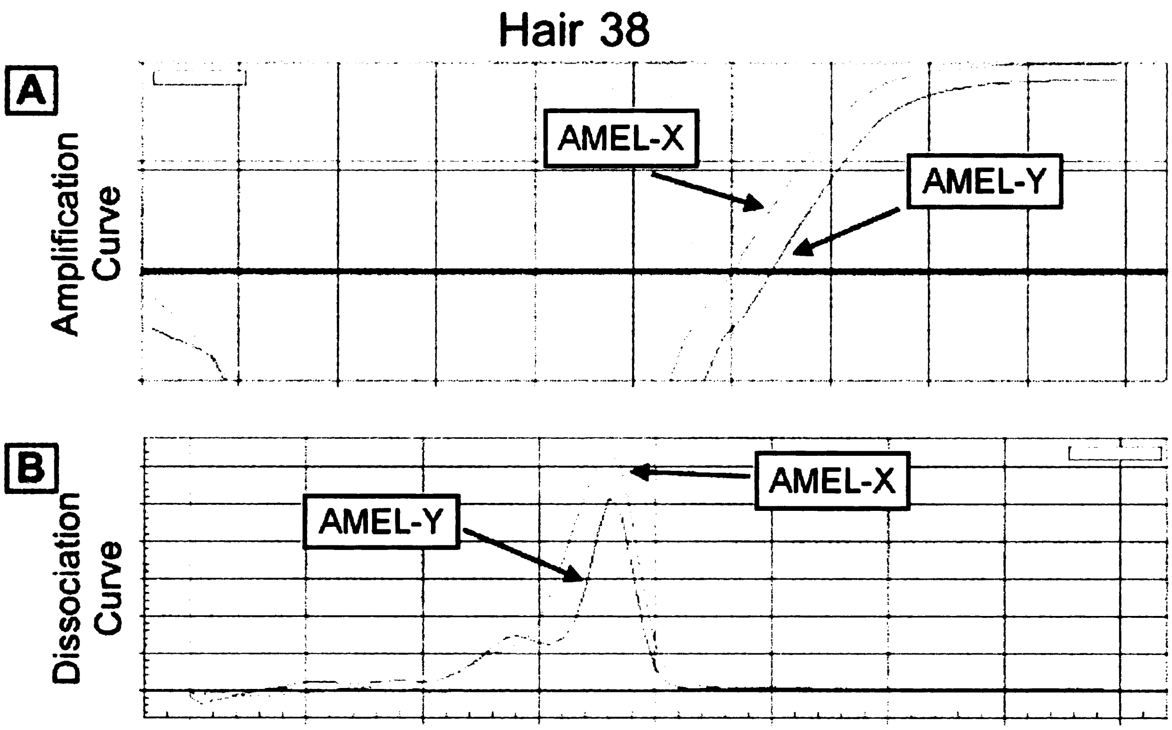

Figure 18: Female Hair 38 Sexing Result using the Amelogenin Assay
Hair 38 typed as male when the known sex was female. (A) The AMEL-X and AMEL-Y amplification plots (x-axis = cycle number, y-axis = RFU value). Both amplification curves crossed the threshold of 10 RFUs (bold line). The AMEL-X Ct value was 30 cycles and the AMEL-Y Ct value was 32 cycles. (B) The AMEL-X and AMEL-Y peaks on the dissociation curve were at the correct temperatures (x-axis = temperature (°C), y-axis = -d(RFU)/dT, AMEL-X and AMEL-Y melt temperature = 73.5°C).

Hairs 17 and 55 incorrectly sexed as female using the amelogenin assay. Amplification and dissociation curves for one replicate from both are illustrated in Figures 19 and 20, respectively. For hair 17, only the AMEL-X product yielded an amplification curve that crossed the threshold and a dissociation curve at the correct temperature. No curve was present for the AMEL-Y product (Figure 19). Hair 55 generated an amplification curve for AMEL-X and a non-sigmoidal curve for AMEL-Y. The dissociation curve of the AMEL-X product produced a peak at the correct temperature, but the peak for the AMEL-Y dissociation curve was too low (Figure 20).

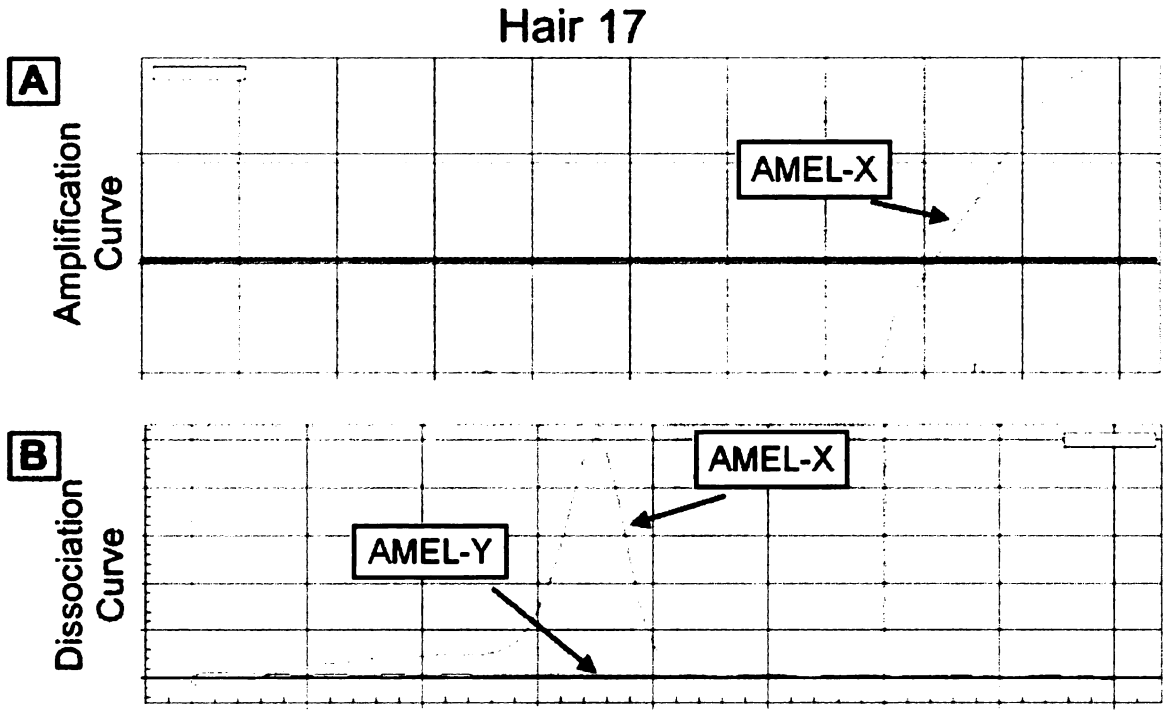

Figure 19: Male Hair 17 Sexing Result using the Amelogenin Assay
Hair 17 typed as female when the known sex was male. (A) The AMEL-X amplification curve (x-axis = cycle number, y-axis = RFU value). Only AMEL-X produced an amplification curve that crossed the threshold (bold line) at a Ct value of 41 cycles. (B) The AMEL-X peak on the dissociation curve was at the correct temperature (x-axis = temperature (°C), y-axis = -d(RFU)/dT, AMEL-X melt temperature = 73.5°C). No signal was produced for AMEL-Y.

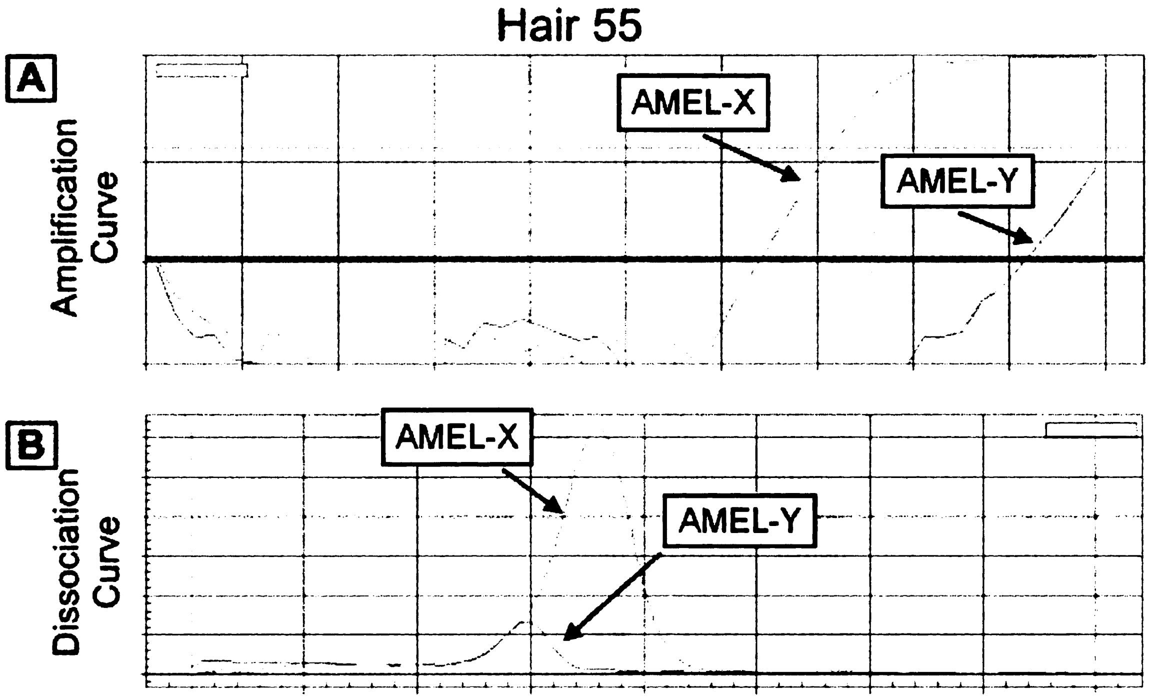

Figure 20: Male Hair 55 Sexing Result using the Amelogenin Assay
Hair 55 typed as female when the known sex was male. (A) The AMEL-X and AMEL-Y amplification curve (x-axis = cycle number, y-axis = RFU value). AMEL-X and AMEL-Y produced an amplification curve that crossed the threshold of 10 RFUs (bold line). The AMEL-X Ct value was 32 cycles and the AMEL-Y Ct value was 46 cycles. Note the non-sigmoidal curve and the high Ct value of the AMEL-Y signal. (B) The AMEL-X peak on the dissociation curve was at the correct temperature, while the AMEL-Y peak was at a temperature too low for sex determination (x-axis = temperature (°C), y-axis = -d(RFU)/dT, AMEL-X melt temperature = 73.5°C, AMEL-Y melt temperature = 70°C).

DYZ1/Alu Assay

Twenty-eight hairs (93%), 20 female and 8 male, matched the known sex when analyzed using the DYZ1/Alu assay. No hairs were incorrectly typed female or were considered inconclusive. An incorrect sexing result was made for hair 35 and 56 using organically extracted DNA. When the DNA from the alkaline digestion was analyzed, both hair 35 and 56 yielded the correct female sexing result. An incorrect male sex result was obtained from hairs 19 and 28 using DNA from both the organic extraction and the alkaline digestion techniques. Hair 19 produced a signal for both Alu and DYZ1 that crossed the threshold; however the Ct values were 15 cycles apart for both the organic extraction and alkaline digestion (Figure 21). DNA organically extracted from Hair 28 produced a signal that crossed the threshold for Alu and non-sigmoidal curve for DYZ1 (Figure 22). The alkaline digestion technique yielded DNA that produced a signal for both Alu and DYZ1 that crossed the threshold; however the Ct values were 15 cycles apart.

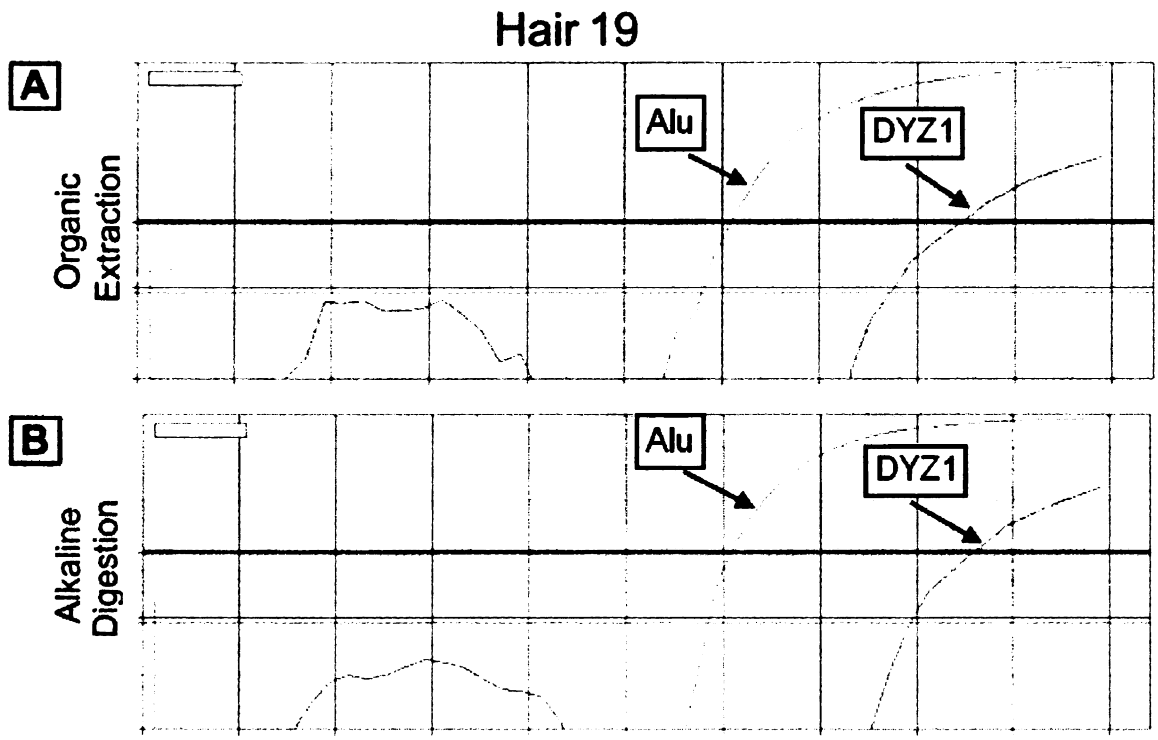

Figure 21: Female Hair 19 Sexing Result using the DYZ1/Alu Assay
The DYZ1 and Alu products were present in the DNA from the (A) organic extraction and (B) alkaline digestion of hair 19. (x-axis = cycle number, y-axis = RFU values). The bold line represents the threshold value of 10 RFUs. The DYZ1 Ct value for the organic extraction was 42 cycles, while the Alu Ct value was 31 cycles. For the alkaline digestion, the Alu Ct value was 31 cycles and the DYZ1 Ct value was 43 cycles. Note the large separation of Ct values for Alu and DYZ1 for both isolation techniques.

Hair 28

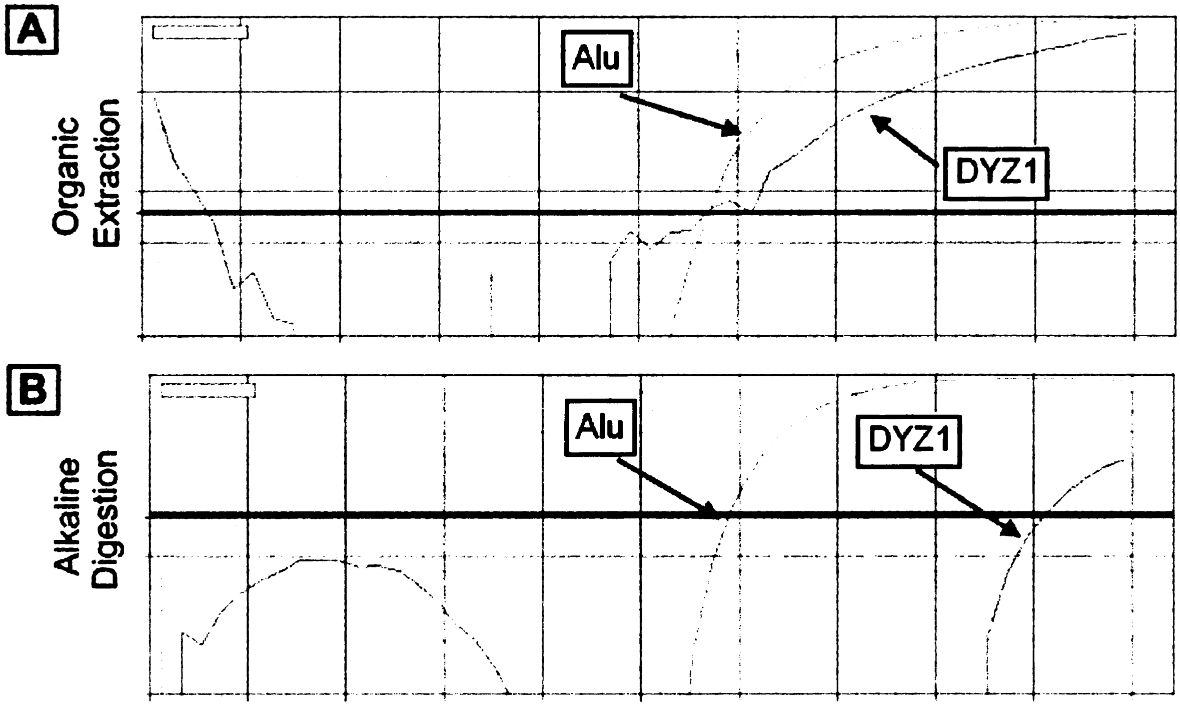

Figure 22: Female Hair 28 Sexing Result using the DYZ1/Alu Assay
The DYZ1 and Alu products were present in the DNA from the (A) organic extraction and (B) alkaline digestion of hair 28. (x-axis = cycle number, y-axis = RFU values). The bold line represents the threshold value of 10 RFUs. The DYZ1 and Alu Ct value for the organic extraction was 28 cycles. For the alkaline digestion, the DYZ1 Ct value was 46 cycles and the Alu Ct value was 29 cycles. Note the non-sigmoidal curve for the DYZ1 signal of the organic extraction and the separation of Ct values for Alu and DYZ1 of the alkaline digestion.

Ancient Skeletal Sexing Results

Table 7 displays the sexing results and anthropological sex estimations for the Butrint and Kamenica, Albania adult skeletal remains. Two or three bones were analyzed per individual.

Table 7: Molecular Sexing Results and Anthropological Sex for Ancient Adult Bones

Sexing results using the amelogenin and DYZ1/Alu assays were compared to the anthropological estimated sex for the Butrint, Albania (BA) and Kamenica, Albania (KA) adult skeletal samples. An asterisk (*) represents results that do not match the anthropologically estimated sex. An inconclusive result was given to bones when a sex determination could not be made.

Bone Identifier	Specific Bone	Amelogenin Assay	DYZ1/Alu Assay	Anthropological Sex
BA Adults				
1187.1	right radius midshaft	inconclusive	male	male
1187.2	right fibula midshaft	inconclusive	male	male
1226.1	right fibula	inconclusive	male	male
1226.2	left ulna midshaft	female*	male	male
1236.1	fibula midshaft	inconclusive	female	female
1236.2	left ulna midshaft	inconclusive	female	female
1518.1	humeral cortical frag	inconclusive	female*	male
1518.2	fibula midshaft	female*	male	male
5010.1	fibula midshaft	inconclusive	female	female
5010.2	humerus midshaft	inconclusive	female	female
3023.1	petrous portion	inconclusive	male	male
KA Adults				
66	humerus	inconclusive	male	male
66	femur	inconclusive	male	male
75	tibia	inconclusive	male	male
75	femur	inconclusive	male	male
75	petrous portion	male	male	male
82	radius	inconclusive	male	male
82	petrous portion	male	male	male
85	femur	inconclusive	male	male
97	tibia	male	female*	male
97	femur	female*	male	male
102	humerus	female	female	female
102	petrous portion	inconclusive	female	female
104	humerus	inconclusive	male	male
104	femur	inconclusive	male	male
142	pelvis	inconclusive	female*	male
142	petrous portion	inconclusive	male	male
142	humerus	female*	male	male
156	femur	female*	female*	male
156	petrous portion	inconclusive	female*	male
156	humerus	female*	male	male

Adult Butrint Skeletal Remains

Six individuals were analyzed from the Butrint adult skeletal remains (Table 7). Two bones were analyzed per individual, except 3023 where only DNA from the petrous portion was available. The amelogenin assay produced no results for nine of the bones, while individuals 1226 and 1518 demonstrated bones that sexed as female, the 1226 left ulna midshaft and the 1518 fibula midshaft, while the anthropologically estimated sex was male. The amplification and dissociation curves for individuals 1226 and 1518 are illustrated in Figures 23 and 24, respectively. Only an amplification curve for AMEL-Y crossed the threshold (Figure 23A), while no dissociation curve was present for either product for the 1226 right fibula (Figure 23B). The left ulna midshaft produced an amplification curve that crossed the threshold for both AMEL-X and AMEL-Y (Figure 23C), but only the peak for the AMEL-X dissociation curve was at the correct temperature (Figure 23D). The AMEL-Y dissociation curve was approximately ten degrees higher than the correct temperature. The 1518 humeral cortical fragment amelogenin sexing results demonstrated an amplification curve that barely crossed the threshold for both the AMEL-X and AMEL-Y products (Figure 24A), but neither product displayed a dissociation curve (Figure 24B). Only the AMEL-X product produced a signal that crossed the threshold and a correct melting temperature for bone 1518 fibula midshaft (Figure 24 C and D).

Figure 23: Sexing Results for Burial 1226 using the Amelogenin Assay
The anthropological sex for burial 1226 was male. The right fibula produced no sexing result and the left ulna midshaft typed as female. (A) The amplification plot for 1226 right fibula (x-axis = cycle number, y-axis = RFU value, AMEL-Y Ct value = 47 cycles). The bold line represents the threshold value of 10 RFUs. (B) The dissociation curve for 1226 right fibula. Neither product produced a dissociation curve (x-axis = temperature (°C), y-axis = -d(RFU)/dT). (C) The amplification plot for 1226 left ulna midshaft (x-axis = cycle number, y-axis = RFU value, AMEL-X Ct value = 41 cycles, AMEL-Y Ct value = 37 cycles). The bold line represents the threshold value of 10 RFUs. (D) The dissociation curve for 1226 left ulna midshaft (x-axis = temperature (°C), y-axis = -d(RFU)/dT, AMEL-X melt temperature = 73.5°C, AMEL-Y melt temperature = 85.5°C). Note the dissociation curve for AMEL-Y 10 degrees higher than the correct temperature.

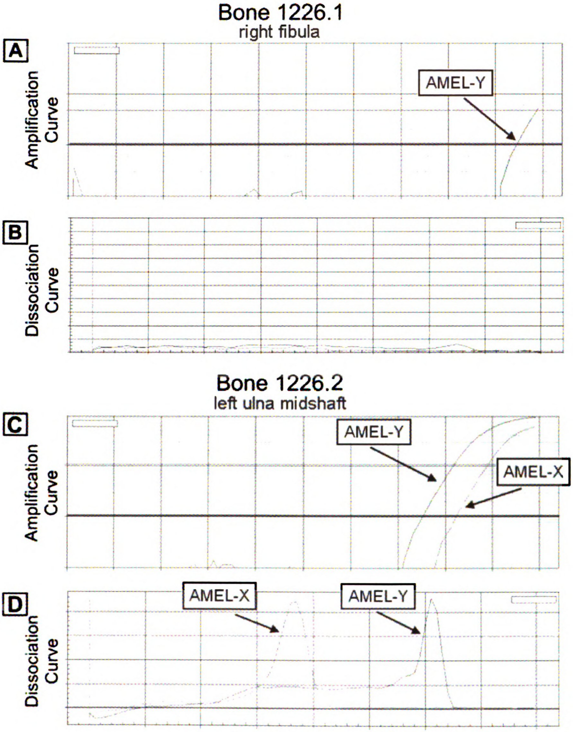
Bone 1226.1
right fibula
A
Amplification Curve
AMEL-Y
B
Dissociation Curve
Bone 1226.2
left ulna midshaft
C
Amplification Curve
AMEL-Y
AMEL-X
D
Dissociation Curve
AMEL-X
AMEL-Y

Figure 24: Sexing Results for Burial 1518 using the Amelogenin Assay
The anthropological sex for burial 1518 was male. The humeral cortical fragment produced no sexing results and the fibula midshaft typed as female. (A) The amplification plot for 1518 humeral cortical fragment (x-axis = cycle number, y-axis = RFU value). Neither the AMEL-X nor AMEL-Y produced an amplification signal that crossed the threshold of 10 RFUs (bold line). (B) The dissociation curve for 1518 humeral cortical fragment (x-axis = temperature (°C), y-axis = -d(RFU)/dT). (C) The amplification plot for 1518 fibula midshaft (x-axis = cycle number, y-axis = RFU value, AMEL-X Ct value = 39 cycles). The bold line represents the threshold value of 10 RFUs. (D) The dissociation curve for 1518.2 (x-axis = temperature (°C), y-axis = -d(RFU)/dT, AMEL-X melt temperature = 73.5°C).

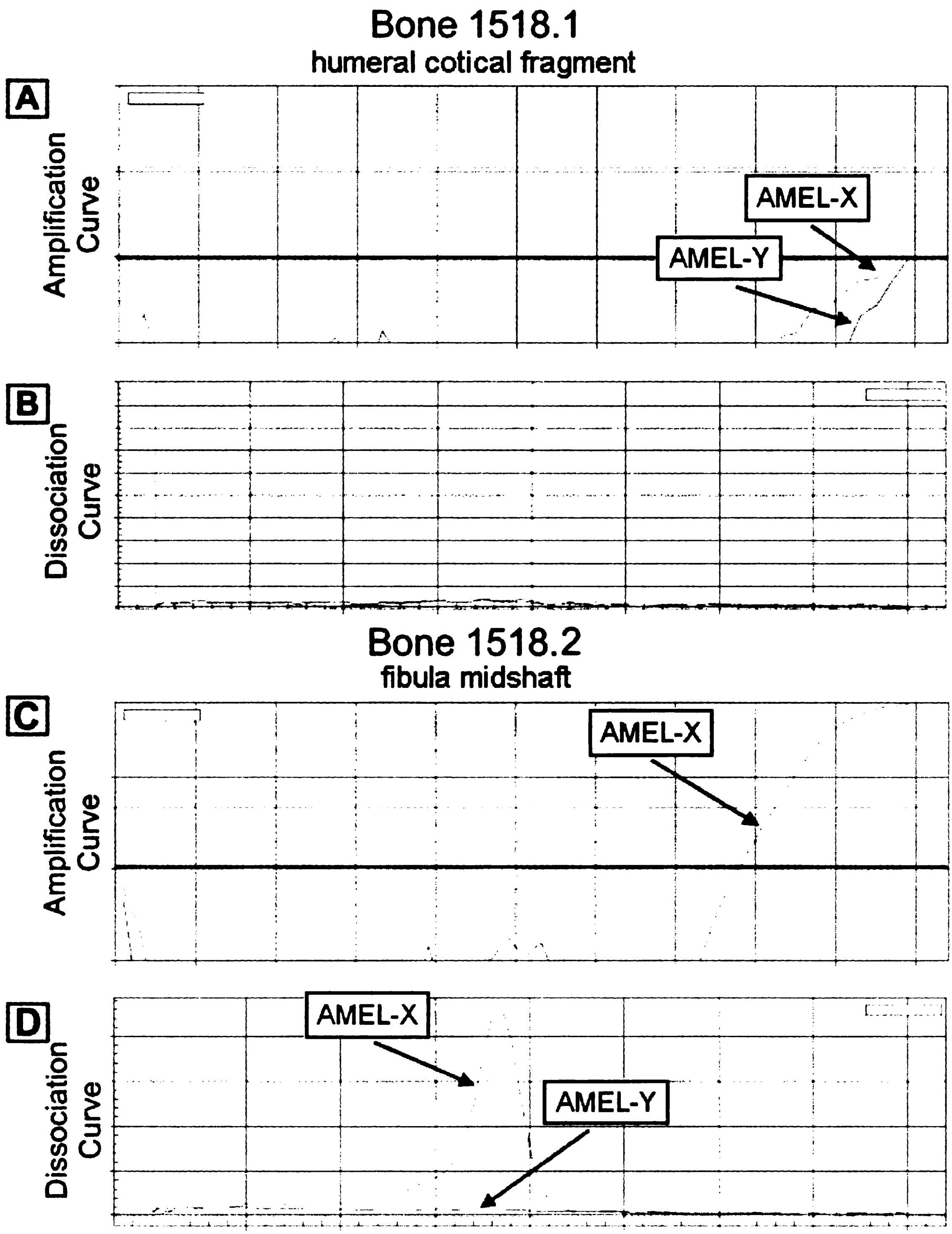
Bone 1518.1
humeral cotical fragment
A
Amplification Curve
AMEL-X
AMEL-Y
B
Dissociation Curve
Bone 1518.2
fibula midshaft
C
Amplification Curve
AMEL-X
D
Dissociation Curve
AMEL-X
AMEL-Y

When analyzed using the DYZ1/Alu assay, all six individuals yielded a sexing result consistent with the anthropological sex, encompassing two females and four males, and no inconclusive results. Bones from each individual demonstrated concordant results, except burial 1518, from which the humeral cortical fragment sexed as female and the fibula midshaft sexed as male. The amplification plots for burial 1518 are illustrated in Figure 25. The Alu product produced a signal that crossed the threshold for bone 1518 humeral cortical fragment, while the DYZ1 curve was well below the threshold (Figure 25A). The fibula midshaft of burial 1518 demonstrated an amplification curve that crossed the threshold for both the Alu and DYZ1 products (Figure 25B); however, the DYZ1 Ct value was approximately eight cycles higher than that of Alu.

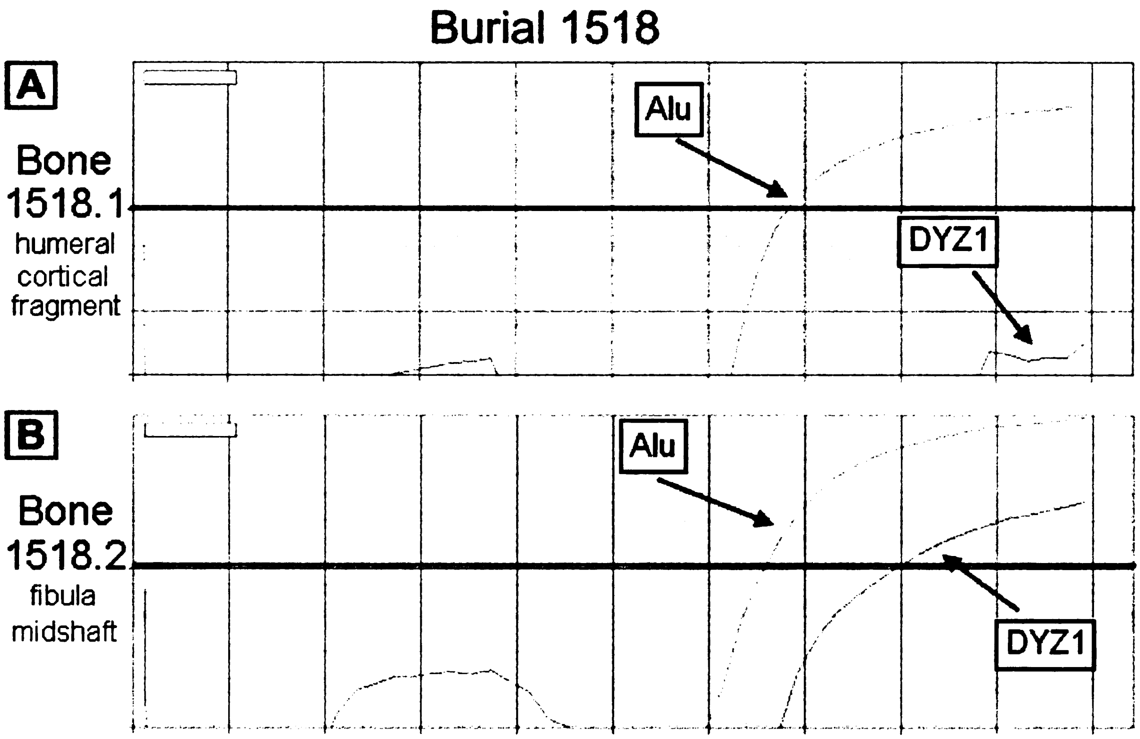

Figure 25: Sexing Results for Burial 1518 using the DYZ1/Alu Assay
The anthropological sex for burial 1518 was male. The humeral cortical fragment typed as female and the fibula midshaft typed as male (x-axis = cycle number, y-axis = RFU values). The bold line represents the threshold value of 10 RFUs. (A) The plot for 1518 humeral cortical fragment demonstrates a signal crossing the threshold for Alu at 39 cycles and a non-sigmoidal curve that does not cross the threshold for DYZ1. (B) The plot for 1518 fibula midshaft demonstrates a curve for both DYZ1 and Alu that crosses the threshold. Note the Ct values differ by approximately eight cycles with the DYZ1 Ct value at 40 cycles and the Alu Ct value at 33 cycles.

Adult Kamenica Skeletal Remains

Nine individuals were analyzed from Kamenica, Albania, using two or three bones sexed from each, except individual 85 where only DNA from a femur was available (Table 7). Twelve out of twenty bones produced no sexing results and of the remaining eight, four typed consistently with the anthropological sex using the amelogenin assay. Four bones did not yield sexing results consistent with the anthropological sex. Individuals 75, 82, and 102 yielded one bone (75 and 82 petrous portion, and 102 humerus) consistent with the anthropological sex, while the remaining bone produced no sexing result. The 75 and 82 petrous portions produced amplification signals for both the AMEL-X and AMEL-Y products that crossed the threshold and dissociation curves at the correct temperatures, thereby typing male (data not shown). The 102 humerus only produced an amplification signal that crossed the threshold and a dissociation curve at the correct temperature for the AMEL-X product, thereby typing female (data not shown). The petrous portion of burials 142 and 156, and 156 femur, sexed as female although the estimated anthropological sex was male. Figure 26A and B shows the result for the petrous portion of burial 142, in which only the AMEL-X product yielded an amplification curve that crossed the threshold and had a dissociation curve at the correct temperature. No signal was detected for the AMEL-Y product. The additional bones sexed from burial 142, the pelvis and humerus, gave no sex result. The pelvis demonstrated no amplification or dissociation curve for either the AMEL-X or AMEL-Y products (Figure 26 C and D). The humerus yielded a signal for AMEL-X and AMEL-Y that crossed the threshold on the amplification plot (Figure 26E), but demonstrated no dissociation curves (Figure 26F).

Figure 26: Sexing Results for Burial 142 using the Amelogenin Assay
The anthropological sex for burial 142 was male. The petrous portion typed as female and the pelvis and humerus produced no sexing results. (A) The amplification plot for 142 petrous portion (x-axis = cycle number, y-axis = RFU value, AMEL-X Ct value = 37 cycles). (B) The dissociation curve for 142 petrous portion (x-axis = temperature (°C), y-axis = -d(RFU)/dT, AMEL-X melt temperature = 75.5°C). (C) The amplification plot for 142 pelvis (x-axis = cycle number, y-axis = RFU value). The bold line represents the threshold value of 10 RFUs. Note that no signal was produced for either AMEL-X or AMEL-Y. (D) The dissociation curve for 142 pelvis (x-axis = temperature (°C), y-axis = -d(RFU)/dT). (E) The amplification plot for 142 humerus (x-axis = cycle number, y-axis = RFU value, AMEL-X Ct value = 7 cycles, AMEL-Y Ct value = 12 cycles). The bold line represents the threshold value of 10 RFUs. Note that neither AMEL-X nor AMEL-Y produced sigmoidal curves (F) The dissociation curve for 142 humerus (x-axis = temperature (°C), y-axis = -d(RFU)/dT).

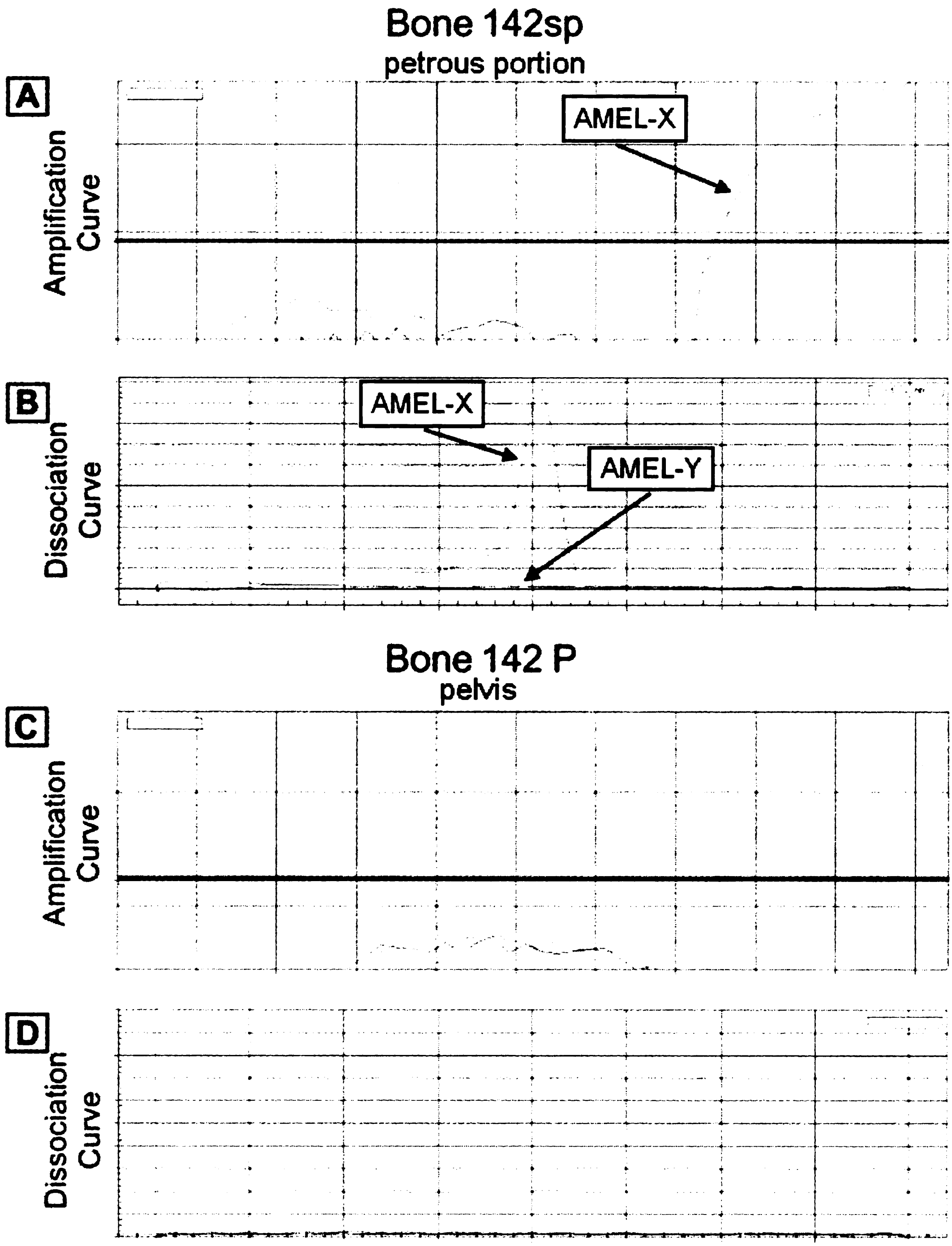
Bone 142sp
petrous portion
A
Amplification Curve
AMEL-X
B
Dissociation Curve
AMEL-X
AMEL-Y
Bone 142 P
pelvis
C
Amplification Curve
D
Dissociation Curve

Figure 26 (cont'd)

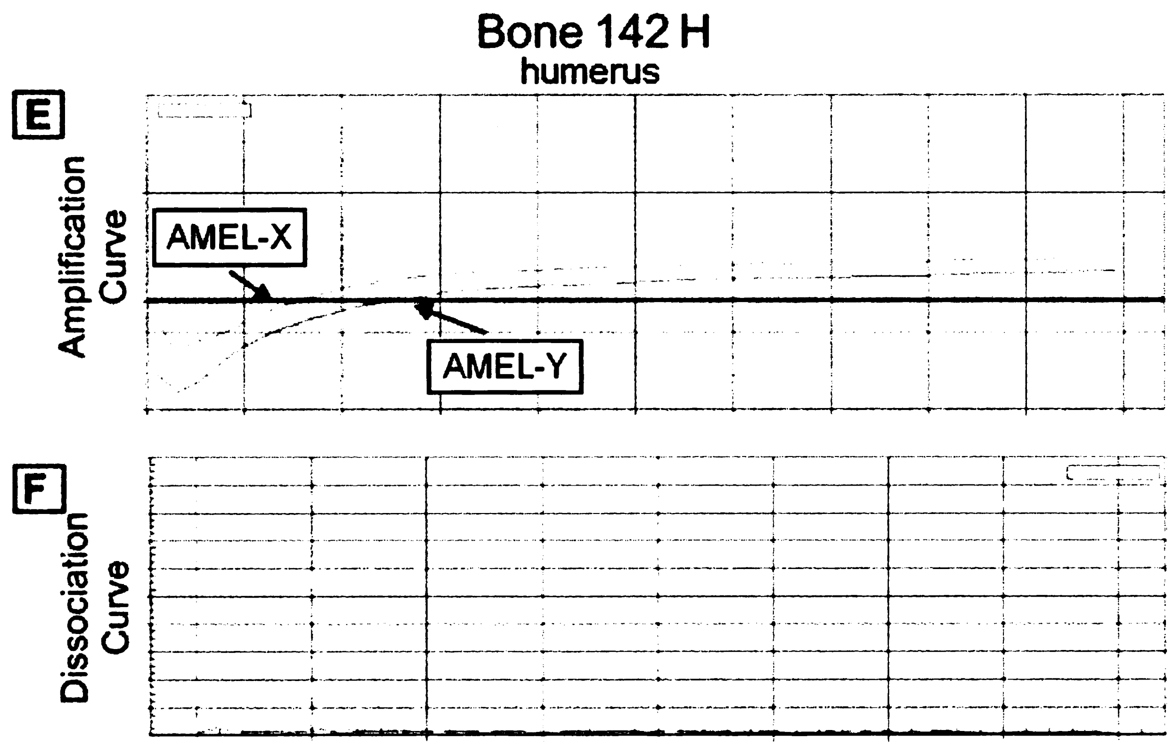

Sexing results for the all bones of burial 156 are presented in Figure 27. The femur demonstrated an AMEL-X amplification curve barely crossing the threshold and a small dissociation curve at the correct melt temperature. The AMEL-Y product yielded a non-sigmoidal curve that produce a very low Ct value and no dissociation curve (Figure 27 A and B). The sexing result for the petrous portion yielded only an amplification curve that crossed the threshold and dissociation curve at the correct temperature for AMEL-X (Figure 27 C and D). The additional bone for burial 156, the humerus produced no amplification or dissociation curve for either the AMEL-X or AMEL-Y product (Figure 27 E and F) and no sex result could be determined.

Figure 27: Sexing Results for Burial 156 using the Amelogenin Assay
The anthropological sex for burial 142 was male. The femur and petrous portion typed as female and the humerus produced no sexing result. (A) The amplification plot for 156 femur (x-axis = cycle number, y-axis = RFU value, AMEL-X Ct value = 10 cycles, AMEL-Y Ct value = 48 cycles). The AMEL-Y produced a non-sigmoidal curve and the AMEL-X produced a signal barely crossing the threshold (bold line). (B) The dissociation curve for 156 femur (x-axis = temperature (°C), y-axis = -d(RFU)/dT, AMEL-X melt temperature = 75.5°C). Note the small dissociation curve for AMEL-X at the correct temperature. (C) The amplification plot for 156 petrous portion (x-axis = cycle number, y-axis = RFU value, AMEL-X Ct value = 36 cycles). The bold line represents the threshold value of 10 RFUs. No signal was produced for the AMEL-Y product. (D) The dissociation curve for 156 petrous portion (x-axis = temperature (°C), y-axis = -d(RFU)/dT, AMEL-X melt temperature = 75.5°C). (E) The amplification plot for 156 humerus (x-axis = cycle number, y-axis = RFU value). Note that neither AMEL-X nor AMEL-Y produced sigmoidal amplification curves. The bold line represents the threshold value of 10 RFUs. (F) The dissociation curve for 156 humerus (x-axis = temperature (°C), y-axis = -d(RFU)/dT).

Bone 156 F
femur

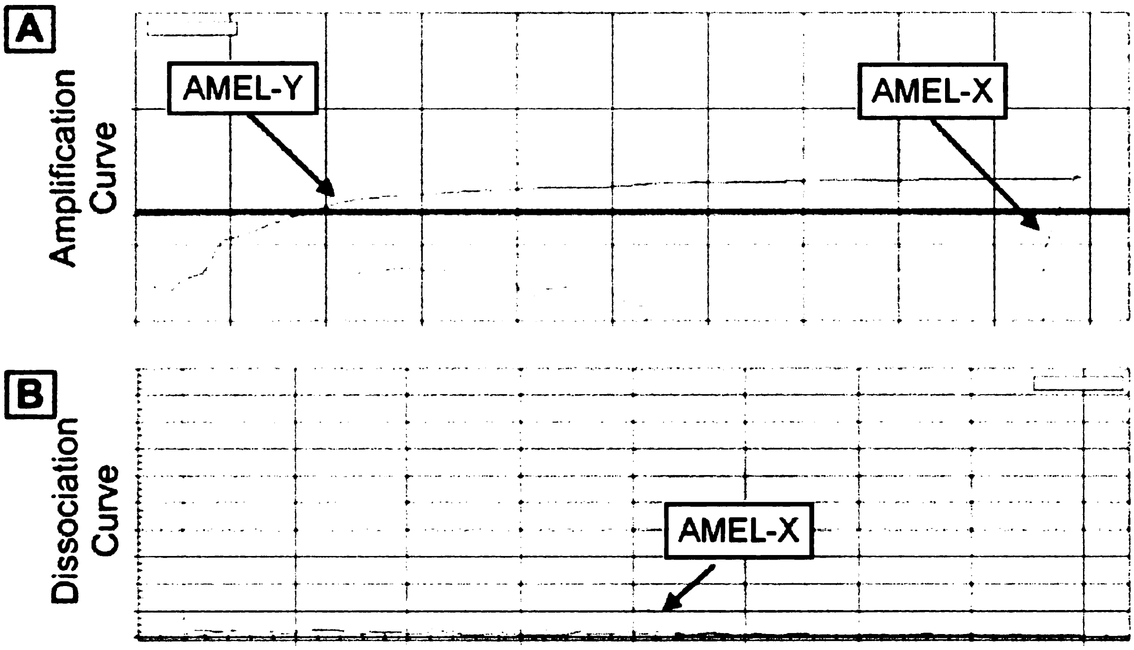

Bone 156sp
petrous portion

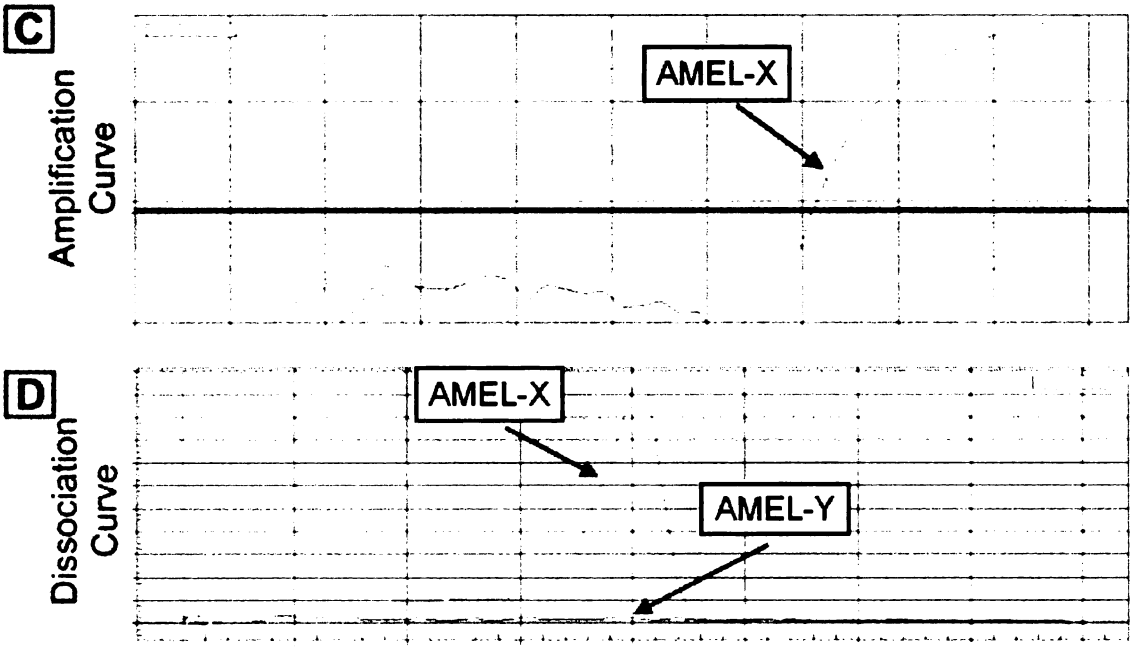

Figure 27 (cont'd)

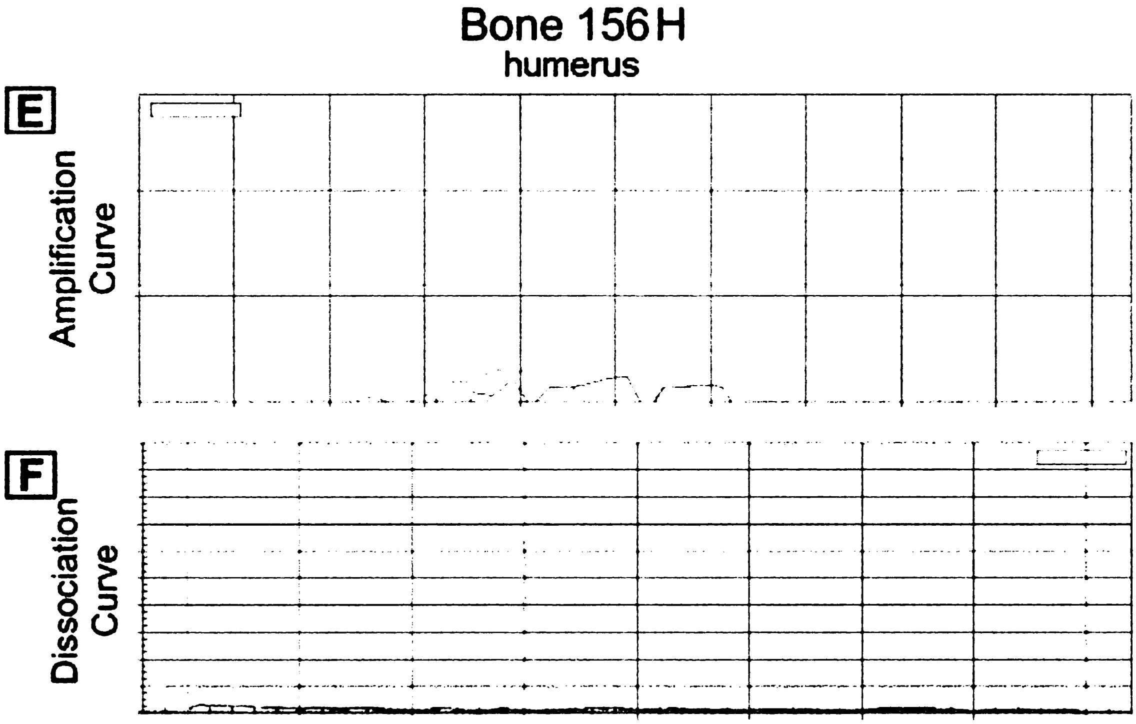

The tibia of burial 97 typed as male, while the femur generated a female result (Figure 28). Both the AMEL-X and AMEL-Y products produced an amplification curve that crossed the threshold for the 97 tibia (Figure 28A), along with dissociation curves at the correct temperature (Figure 28B). The 97 femur yielded only the AMEL-X product that presented an amplification curve that crossed the threshold (Figure 28C) and a dissociation curve at the correct temperature (Figure 28D).

Figure 28: Sexing Results for Burial 97 using the Amelogenin Assay
The anthropological sex for burial 97 was male. The tibia was typed as male and the femur was typed as female. (A) The amplification plot for 97 tibia (x-axis = cycle number, y-axis = RFU value, AMEL-X Ct value = 29 cycles, AMEL-Y Ct value = 39 cycles). The bold line represents the threshold value of 10 RFUs. Note the Ct values are different by 10 cycles. (B) The dissociation curve for 97 tibia (x-axis = temperature (°C), y-axis = -d(RFU)/dT, AMEL-X melt temperature = 75.5°C, AMEL-Y melt temperature = 75°C). (C) The amplification plot for 97 femur (x-axis = cycle number, y-axis = RFU value). The bold line represents the threshold value of 10 RFUs. An amplification curve crossed the threshold for AMEL-X product at 39 cycles and no curve crossed the threshold for the AMEL-Y. (D) The dissociation curve for 97 femur (x-axis = temperature (°C), y-axis = -d(RFU)/dT, AMEL-X melt temperature = 74°C).

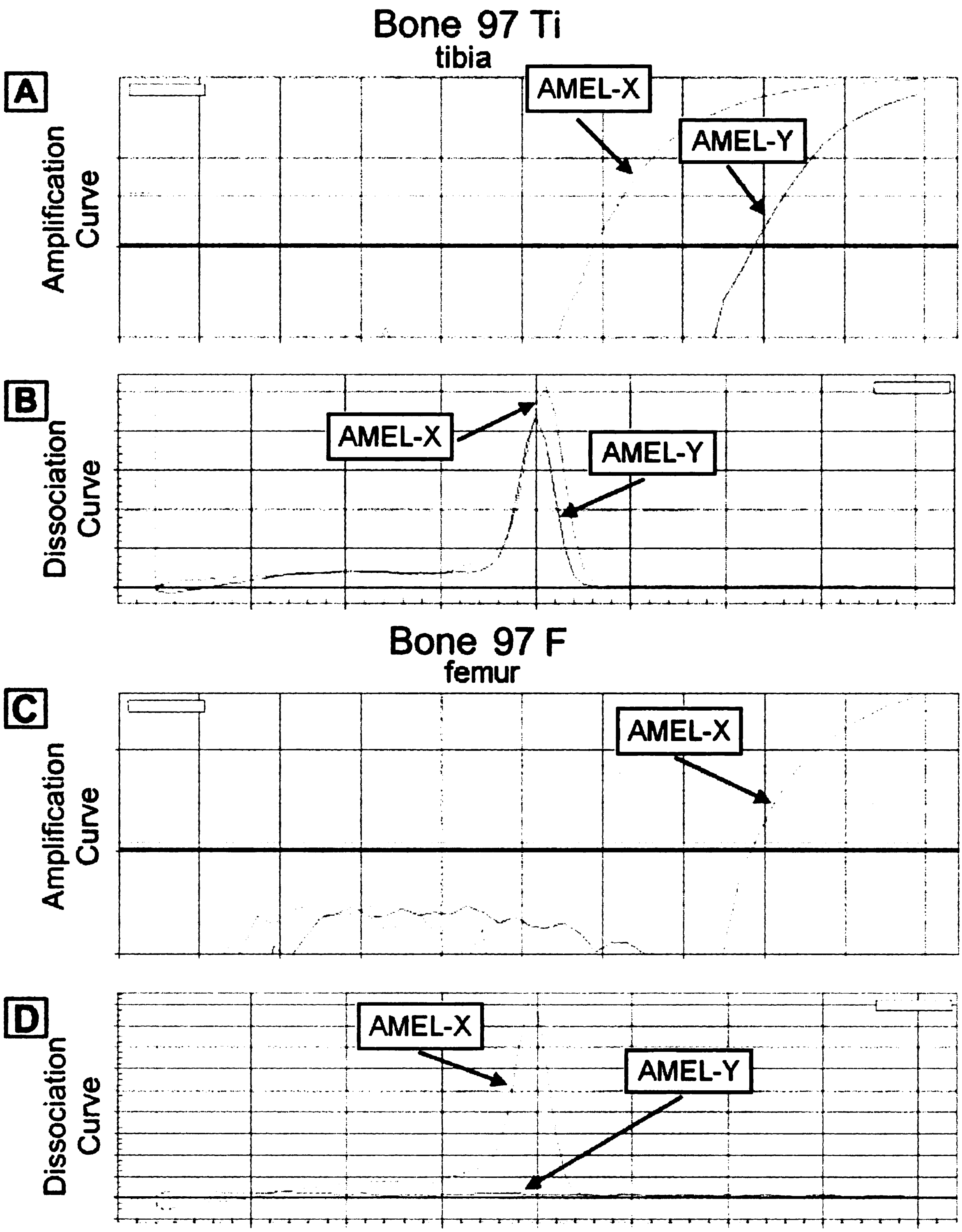
Bone 97 Ti
tibia
A
Amplification Curve
AMEL-X
AMEL-Y
B
Dissociation Curve
AMEL-X
AMEL-Y
Bone 97 F
femur
C
Amplification Curve
AMEL-X
D
Dissociation Curve
AMEL-X
AMEL-Y

DYZ1/Alu sexing results from all nine adult Butrint individuals, one female and eight males, were consistent with the anthropological sex estimate. The multiple bones analyzed from five individuals (66, 75, 82, 102, 104) yielded consistent sexing results. The three remaining individuals each had one or more bones (97 tibia, 142 pelvis, and 156 femur and humerus) that typed as female, while the other bones (97 femur, 142 humerus and petrous portion, and 156 petrous portion) typed as male. Figure 29 displays the sexing result for the tibia and femur from burial 97. The tibia only yielded an amplification curve crossing the threshold for the Alu product (Figure 29A) and the femur yielded both the Alu and DYZ1 products (Figure 29B). The sexing results for burial 142 are illustrated in Figure 30. The pelvis yielded only an Alu amplification curve that crossed the threshold (Figure 30A), while the humerus and the petrous portion demonstrated a curve for both DYZ1 and Alu products that crossed the threshold (Figure 30 B and C). In addition, the sexing results from burial 156 are shown in Figure 31. The femur yielded only an amplification curve for the Alu product that crossed the threshold. The DYZ1 signal was below the threshold (Figure 31A). The humerus produced an amplification curve crossing the threshold for only the Alu product (Figure 31B), while both the Alu and DYZ1 produced a signal that crossed the threshold for the petrous portion (Figure 31C).

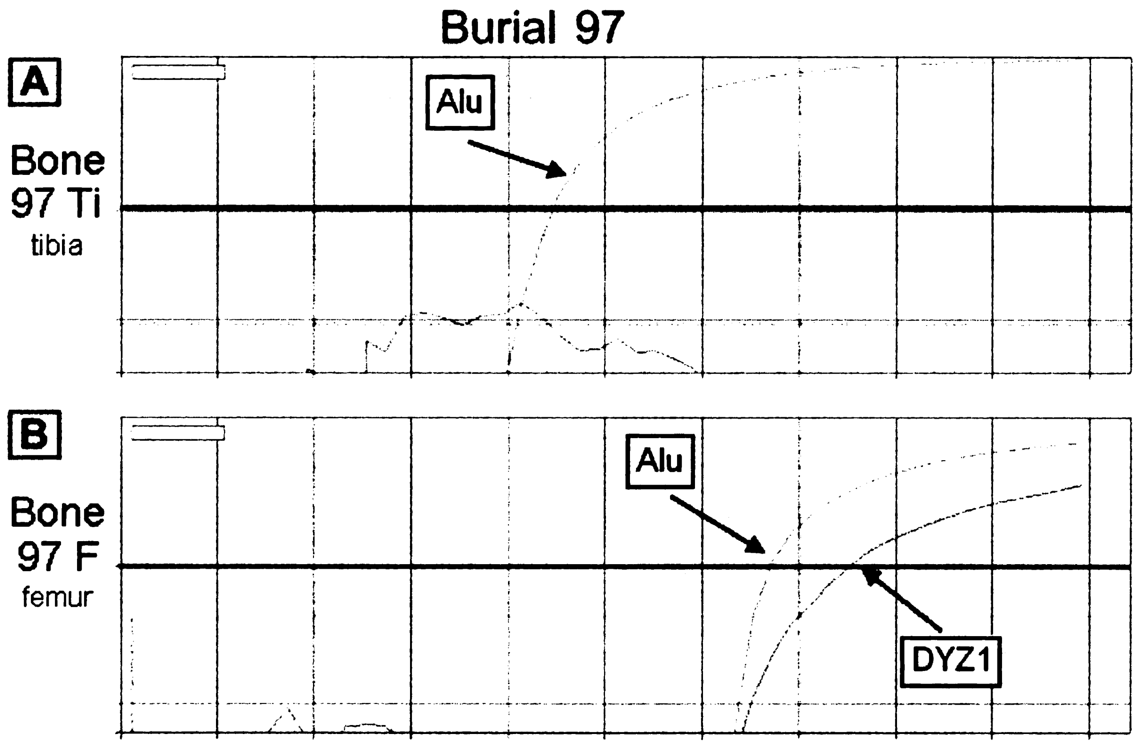

Figure 29: Sexing Results for Burial 97 using the DYZ1/Alu Assay
The anthropological sex for burial 97 was male. The tibia typed as female and the femur typed as male. The bold line represents the threshold value of 10 RFUs (x-axis = cycle number, y-axis = RFU values). (A) The plot for 97 tibia demonstrates a signal crossing the threshold for Alu at 23 cycles and no signal for DYZ1. (B) The plot for 97 femur demonstrates a curve crossing the threshold for both DYZ1 and Alu with a difference in Ct values of five cycles (DYZ1 Ct value = 38 cycles, Alu Ct value = 33 cycles).

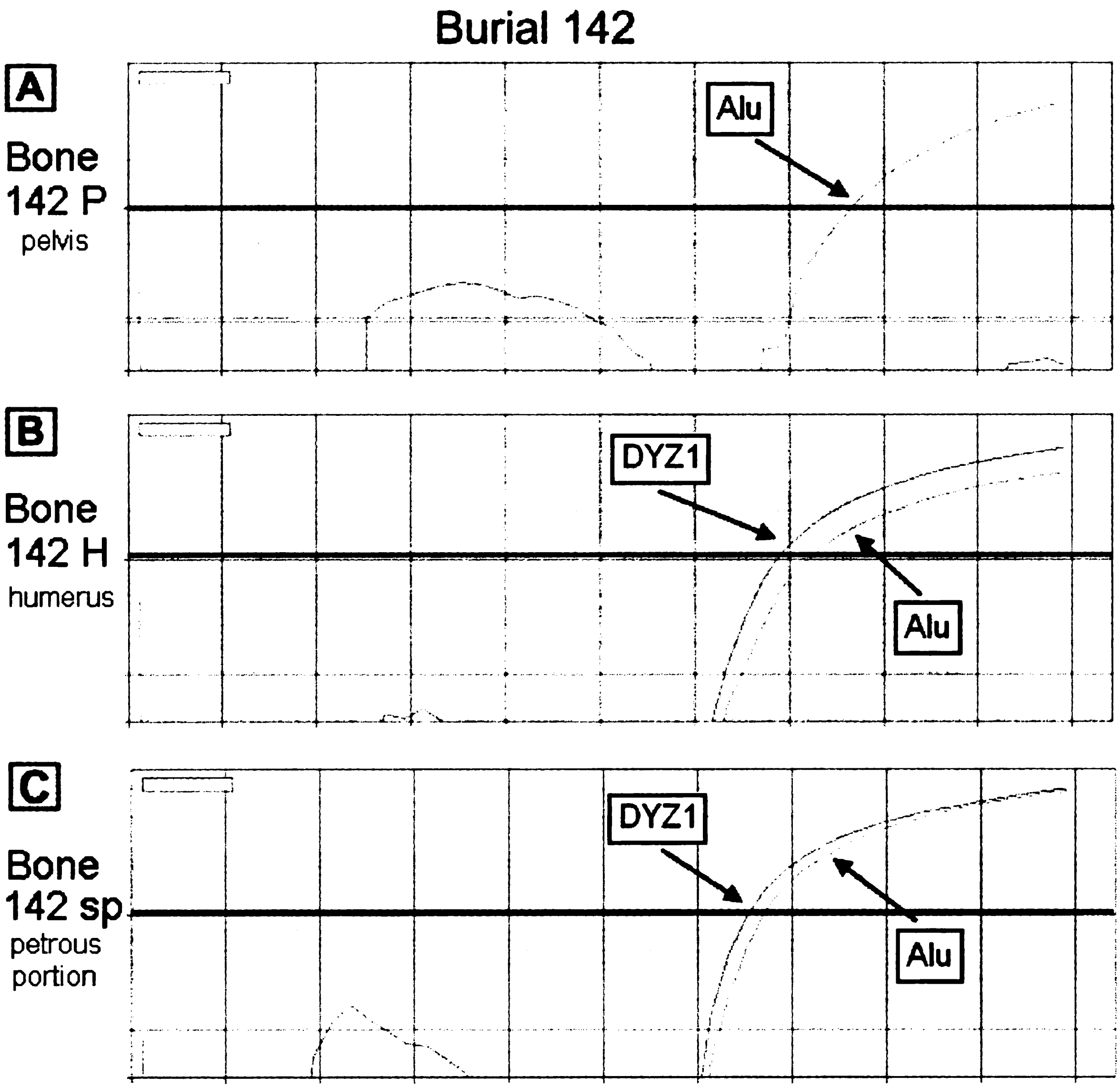

Figure 30: Sexing Results for Burial 142 using the DYZ1/Alu Assay
The anthropological sex of burial 142 was male. The pelvis typed as female and the humerus and petrous portion typed as male (x-axis = cycle number, y-axis = RFU values). The bold line represents the threshold value of 10 RFUs. (A) The plot for 142 pelvis demonstrates a curve for Alu that crosses the threshold at 36 cycles and no curve for DYZ1. (B) The plot for 142 humerus demonstrates a signal crossing the threshold for both DYZ1 and Alu at 34 and 36 cycles, respectively. (C) The plot for 142 petrous portion demonstrates a signal crossing the threshold for both DYZ1 and Alu at 32 and 33 cycles respectively.

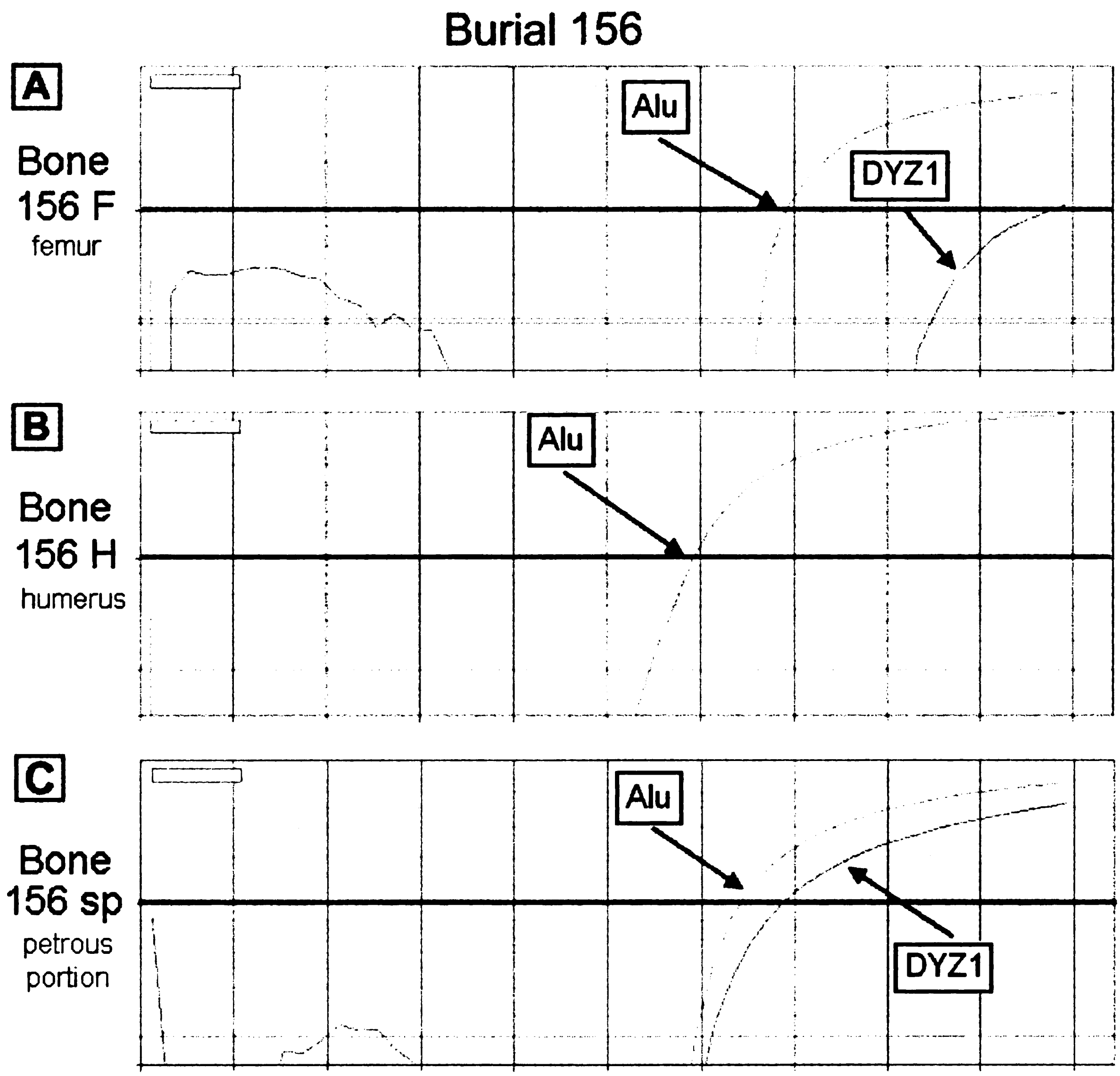

Figure 31: Sexing Results for Burial 156 using the DYZ1/Alu Assay
The anthropological sex for burial 156 was male. The femur and humerus typed as female and the petrous portion typed as male (x-axis = cycle number, y-axis = RFU values). The bold line represents the threshold value of 10 RFUs. (A) The plot for 156 femur demonstrates a signal crossing the threshold for Alu at 34 cycles, but the DYZ1 curve did not cross the threshold. (B) The plot for 156 humerus demonstrates a curve for Alu crossing the threshold at 29 cycles and no curve for DYZ1. (C) The plot for 156 petrous portion demonstrates a signal crossing the threshold for both DYZ1 and Alu at 34 and 32 cycles, respectively.

Juvenile Butrint Skeletal Remains

Seven juveniles from Butrint that could not be sexed anthropologically were sexed molecularly using the amelogenin and DYZ1/Alu assays (Table 8). One bone from juvenile burials 1185, 1225, 1229, and 1259, and two bones from 1224 and 1264, were analyzed.

Table 8: Sexing Results for Butrint, Albania Juvenile Skeletal Samples
Sexing results from the amelogenin and the DYZ1/Alu assays are compared for the Butrint, Albania (BA) juvenile skeletal samples. The asterisk (*) signifies sexing results that did not match the alternate bone for the same individual. An inconclusive result was given to bones where a sex result could not be determined.

Bone Identifier	Specific Bone	Amelogenin Assay	DYZ1/Alu Assay
BA Juveniles			
1185.1	fibula shaft	inconclusive	male
1188.1	left humerus shaft	inconclusive	female*
1188.2	right petrous portion	inconclusive	male*
1224.1	left petrous portion	inconclusive	female
1224.2	right humerus midshaft	female	female
1225.1	right petrous portion	inconclusive	female
1229.2	humeral shaft	inconclusive	male
1259.1	left femur midshaft	inconclusive	male
1264.1	tibia cortical fragment fr. Distal end	inconclusive	male
1264.2	fibula midshaft	male	male

When sexed using the amelogenin assay, one bone from 1224 and 1264 yielded a sexing result; the rest were inconclusive. Using the DYZ1/Alu assay, juveniles 1224 and 1264 typed as female, while 1185, 1229, 1259, and 1264 typed as male. Results were congruent between both bones from juvenile 1224 and 1264. Juvenile 1188 did not produce two bones the same sexing result, therefore an overall sex determination could not be made (Figure 32). The left humerus shaft yielded an for the Alu product; however, the DYZ1 amplification produced an amplification curve below the threshold (Figure 32A). The right petrous portion demonstrated an amplification curve for both the DYZ1 and Alu products that crossed the threshold (Figure 32B).

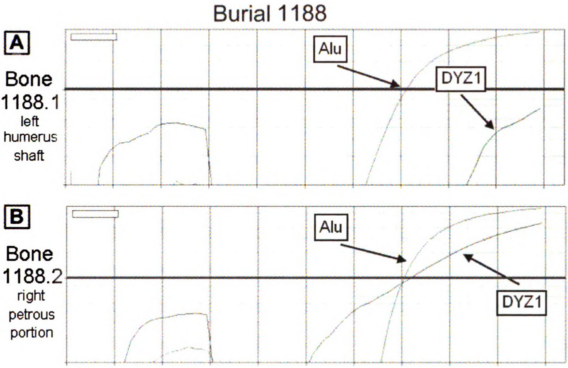

Figure 32: Sexing Results for Burial 1188 using the DYZ1/Alu Assay
Burial 1188 was a juvenile, therefore an anthropological sex could not be determined. The left humerus shaft typed as female and the right petrous portion typed as male (x-axis = cycle number, y-axis = RFU values). The bold line represents the threshold value of 10 RFUs. (A) The plot for 1188 left humerus shaft demonstrated a signal crossing the threshold for Alu at 36 cycles, but the DYZ1 signal did not cross the threshold. (B) The plot for 1188 right petrous portion demonstrated a signal crossing the threshold for Alu and DYZ1 at 36 and 35 cycles, respectively. Note the non-sigmoidal curve of the DYZ1 signal.

DISCUSSION

Generating a physical profile can be extremely important in a forensic investigation of human remains, one foundation of which is accurate sex determination. Standard anthropological sexing methods are generally reliable with high quality materials; however, when remains are incomplete or degraded, molecular sexing techniques may be necessary. In the current study, a more sensitive molecular sexing assay was sought in an attempt to overcome the shortfalls of the standard assay based on the single copy locus amelogenin. The repetitive elements DYZ1 and Alu proved to be a more sensitive sexing tool than amelogenin, both in control assays and when sexing samples of forensic interest such as hair shafts and aged skeletal remains.

Optimization of the amelogenin assay showed that male and female control DNA produced standard amplification curves along with dissociation curves at the correct temperatures for the respective X and Y chromosome products (Figures 11 and 12). This allowed the assay to be used for direct comparison to that with DYZ1 and Alu. Similarly, optimized results for the DYZ1/Alu assay showed standard curves for both loci using control DNA (Figure 13), thereby allowing it to be compared with the amelogenin assay.

While the DYZ1/Alu assay correctly typed male and female control DNA, both markers amplified in some of the negative controls. This was likely caused by contamination resulting from handler DNA on supplies or within reagents, especially primers and probes purchased from venders with unknown quality control procedures. Given this, all supplies and workstations were extensively irradiated to destroy any DNA. In addition, the supermix and primers were irradiated. Periods longer than 30 seconds apparently damaged the primers enough that amplification did not occur, so 30 second irradiation became the standard. The probes were not irradiated because the UV affected the fluorescent dyes such that no signal was detected in the rtPCR reaction (data not shown). Once these precautions were executed, the DYZ1 locus did not amplify in the negative controls; however, the Alu contamination persisted and produced signals that crossed the threshold at 40 cycles or more. Although Alu amplification in the negative control was not ideal, the DYZ1/Alu assay was still viable for unambiguous male sex determination as long as DYZ1 amplified only with male control DNA and not in negative or female controls. Furthermore, the Alu signal for known female DNA crossed the threshold at much lower Ct values than in the negative control, thereby differentiating between a female sexing result and DNA contamination. On the other hand, with extremely low quantities of DNA, an amplification curve could cross the threshold at a high Ct value, making differentiation of contamination and a true female sex result difficult. Therefore, in an actual investigation, such small amounts of DNA would not be reliable for sex determination if contamination existed. When an actual female sample with a high Ct value was observed, additional reactions would need to be performed using an increased amount of DNA to ensure the sex determination was accurate.

Sexing of the DNA dilution series showed that the amelogenin assay was successful using as little HMW DNA as found in approximately 15 cells. Artificial degradation resulted in more than twice as much DNA being required for amplification. These findings make sense given that degradation of the DNA would destroy some of the target loci, thus requiring more input DNA for amplification. This would be the case for forensic samples as well, since DNA found in forensic evidence is often degraded. The

DYZ1/Alu assay was successful using HMW DNA quantities down to 1% of a cell's DNA (0.0623 pg), approximately 1500 times more sensitive than the amelogenin assay. Counterintuitively, the DYZ1/Alu assay was even more sensitive when DNA was artificially degraded, an exact opposite finding of the amelogenin assay. The presumed reason for this is that the DYZ1 repetitive elements are all linked at the heterochromatin region of the Y chromosome (Roewer et al. 1992), therefore acting as a single locus in intact DNA. When analyzing only a few cells' worth of DNA, stochastic sampling effects presumably occurred, in which the DYZ1 region was sometimes sampled and other times it was missed. However, when DNA was degraded, these repeat sequences became fragmented, making it more likely to sample the DYZ1 locus from thousands of repeat copies instead of from one intact sequence. Conversely, the Alu repeat elements are dispersed throughout the genome, making it possible to sample the locus with both HMW and degraded DNA, even at low quantities.

The dilution series of degraded DNA experiments also had several concentrations where DYZ1 amplified in only one replicate. This was likely caused by the lack of optimal digestion of the DYZ1 region, once more resulting in stochastic sampling effects. Further, the DYZ1 locus may not fragment evenly; if the DYZ1 sequence were digested into 10 kb blocks on average, approximately 70 repeats would be linked together, again making stochastic sampling much more likely than with Alu. However, if these repeats were further segmented and dispersed throughout the sample, the target locus would be easier to sample. Conversely, because of the high distribution of Alu repeats, the loci would already be adequately dispersed. This, paired with the slightly higher copy number of Alu repeats, helps explain why the DYZ1 locus did not perfectly mimic Alu amplification, resulting in a difference in their Ct values. The difference could pose a problem when analyzing forensic samples with extremely small amounts of DNA. In this study, a few of the correctly sexed male hairs demonstrated DYZ1 signals with Ct values 5 – 10 cycles higher than the Alu signal (data not shown). Nuclear DNA from hair shafts is highly degraded, but due to the highly compact nature of the Y chromosome heterochromatin region, the DYZ1 sequence may be protected from extensive fragmentation (Roewer et al. 1992), resulting in stochastic sampling and thus the separation of the DYZ1 and Alu Ct values. In contrast, it is also possible that the DYZ1 locus is more susceptible to degradation, resulting in its higher Ct value. Given these findings, analysis of forensic samples with the DYZ1/Alu assay may result in the amplification curves for the two loci being separated more than normal. However, when using control DNA this artifact was only seen when less than 1% of one cell's worth of DNA was assayed. Therefore, seeing such separation may simply indicate that a forensic sample contains an insufficient amount of DNA for definitive sex determination.

Very large amounts of control DNA also produced unanticipated rtPCR results in some instances. Only one replicate amplified both the DYZ1 and Alu for the largest HMW DNA quantity (20000 pg) (Figure 15). The DYZ1 amplification signal crossed the threshold at an extremely low Ct value with a curve that was not sigmoidal, which was likely attributable to the large quantity of DNA itself. If too much DNA is present in PCR reactions, reagents can become limited within the first several cycles resulting in inadequate amplicon production. However, because the DYZ1/Alu assay displayed sigmoidal curves for both loci at similar Ct values at lower DNA quantities, simply diluting the large amount of DNA would produce viable sex determination results.

Comparison of the amelogenin and DYZ1/Alu assays using hair shaft DNA showed that two-thirds analyzed with the amelogenin assay produced X and Y products, and 80% of these yielded a correct sexing result. The remaining third generated either no product or produced a signal for both loci with incorrect dissociation temperatures, resulting in no sex call (e.g., Figure 16). Furthermore, two DNAs typed as male when the donor was female, both of which demonstrated what seemed to be reasonable amplification and dissociation curves (Figure 17 and 18). A possible explanation for this was cross contamination between other samples in the reaction set. However, if contamination was the cause, the Ct values would presumably be far apart, but in both cases similar amelogenin Ct values were observed, meaning contamination was unlikely. A sample mix-up when setting up the reaction would also explain the incorrect results, but the hairs typed correctly using the DYZ1/Alu assay, as detailed below. Additionally, two hairs analyzed with the amelogenin assay typed as female although the donor was male, generating an X product with a correct dissociation temperature. The dropout of the Y chromosome could be related to amplifying different sized amplicons in highly degraded DNA. Because the amelogenin Y product is larger than the X sequence, assaying an intact copy of it could be more difficult, explaining why a male hair typed as a female.

When hair shaft DNA was analyzed using the DYZ1/Alu assay, all hairs yielded a sexing result. Ninety-three percent of these were correct, or about twice as many as the amelogenin assay. In addition, the four hairs that were incorrectly called with the amelogenin assay produced accurate sexing results with the DYZ1/Alu assay. However, two other hairs were incorrectly sexed as male, as the DYZ1 curve crossing the threshold.

It should be noted that neither of these hairs (19 and 28) were "clean" results. Hair 19 generated a DYZ1 signal with a Ct value 15 cycles higher than the Alu signal (Figure 21), while hair 28 displayed a non-sigmoidal curve for DYZ1 from the organic extraction, along with a Ct value also 15 cycles higher than Alu with the alkaline digestion, making the male results dubious. Potential explanations for these data are that both female donors actually had a Y chromosome, or at least a segment of DNA similar enough to DYZ1 to allow amplification. Schmid et al. (1992) described females who harbored a Y chromosome along with two X chromosomes. However, there have been only five reported cases of XXY females, making it extremely unlikely that two female hair donors displayed this characteristic. Furthermore, because the Alu sequence is not related to the number of X chromosomes, the amplification plot for an XXY female would still present DYZ1 and Alu signals that would cross the threshold at similar Ct values. A more likely explanation is contamination with a small amount of male DNA, which would explain why the DYZ1 amplification curves crossed the threshold much later than the Alu product. In addition, Graffy (2003), who originally purified the hair DNAs, had difficulty analyzing the mitochondrial DNA from Hair 19, in that it had many ambiguous base calls. It appears, owing to the inconsistent mtDNA results and the DYZ1/Alu results, there is a good chance that the female hair DNA sample was contaminated with a small amount of male DNA.

Similar amelogenin and DYZ1/Alu results were seen in assays of the ancient skeletal remains. Amelogenin typing showed just a third of the adult bones yielded a sexing result; four of which were the same as the anthropological estimated sex, and the six bones that were inconsistent typing as female. Most of these demonstrated an X product with a clear sigmoidal amplification curve and a dissociation peak at the correct temperature. One of the inconsistent bones (1226 left ulna midshaft) did produce a Y signal (Figure 23); however, because the dissociation temperature was ten degrees too high, it was not considered to be from the Y product. Similar to the hairs, these bones were highly degraded, potentially making assaying the larger Y target sequence more difficult than the X sequence. In addition, the burial 156 femur had an unusual female result (Figure 27 A and B): the curve from the X product barely crossed the threshold, and did so at an extremely high Ct value, while the Y signal produced a non-sigmoidal amplification curve. Normally these results would be considered inconclusive; however because the X signal did produce a small dissociation peak at the correct temperature, the bone was typed as female for this study. Realistically, it would be impossible to make a definitive sex determination with such data. Burial 97 also had two bones with inconsistent amelogenin sexing results (Figure 28), although neither of these yielded unambiguous data. The tibia showed amplification and dissociation curves consistent with male DNA, but the X and Y Ct values were separated by ten cycles. This makes it hard to determine if the Y signal was from the bone or contamination. The femur, on the other hand, displayed curves consistent with female DNA, but the X curve crossed the threshold at approximately 40 cycles, indicating that only a small amount of the X product amplified, making a definitive sex determination difficult. Due to the unreliability of either sexing result for the tibia and femur, a sex determination would not be possible for this individual.

Only two juvenile bones were sexed using the amelogenin assay. The left ulna midshaft of burial 1224 produced an X signal that crossed the threshold and had a dissociation curve at the correct temperature. Burial 1264 fibula midshaft produced both an X and Y signal that crossed the threshold and yielded dissociation curves at the correct temperature. In contrast, the 1224 left petrous portion and the 1264 tibia cortical fragment did not produce a signal for either locus (data not shown). In a forensic investigation multiple bones from an individual would ideally be assayed to make a definitive sex determination. If only one bone is available, multiple DNA extractions should be performed and analyzed separately to ensure the accuracy of the sex result.

The DYZ1/Alu assay of skeletal remains produced far more robust results. All adult and juvenile bones yielded sexing data, and 84% of the adult remains had sexing results consistent with the anthropological sex, along with five that differed among four burials. Each of the latter group demonstrated clear sigmoidal curves for Alu and no DYZ1 result, thereby typing as female. Furthermore, two or three bones were analyzed for 16 adult and juvenile burials, 11 of which produced consistent sexing results among all bones. Five burials produced inconsistent sexing results, including Kamenica burials (97, 142 and 156). Of these, the 97 tibia, 142 pelvis, and 156 femur and humerus typed as female, while the remaining bones typed as male. One explanation for such findings is that some bones produce better DNA results than others. Edson et al. (2004) discussed the success rate of analyzing mtDNA from different bone types. Weight-bearing bones, such as the tibia, have the densest cortical material and generated the best DNA results (approximately 90%), while spongy bones, such as the pelvis, demonstrated a success rate of approximately 65%. This could explain why only Alu amplified from the 142 pelvis, while both loci amplified from the humerus and petrous portion DNAs. However, because both the tibia and femur are weight-bearing bones, it is unlikely that the inconsistent sexing results for burial 97 and 142 were caused by the difference in bone density. A second explanation for inconsistent sexing results is that the bones were not actually from the same individual. The Kamenica tumulus includes double burials (Bejko et al. 2006) several of which were analyzed by Clemmer (2005). In those burials it was clear that two sets of skeletal remains were present. However, many of the Kamenica burials contained only fragmented remains. If skeletal fragmentation is high enough and the bulk of the bones are missing, it would be difficult or in some instances impossible to determine if remains were from one or more than one individuals. Likewise, the nature of a burial mound means that graves occur over other graves, and that commingling may happen over time, either during subsequent burials as the ground shifts, or as the skeletons are unearthed. For example, by observing the diagram of burials 142 and 156 (Figure 33) from the Kamenica map of the lower level of the tumulus, neither burial depicts a full, undisturbed skeleton. It seems plausible that bones from two individuals were unknowingly collected from a grave, accounting for the inconsistent sexing results.

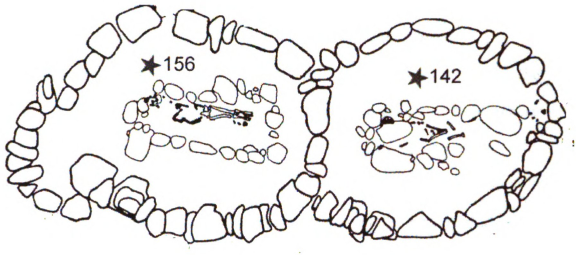

Figure 33: Magnified View of Burials 142 and 156
Partial skeletons of burials 142 and 156 from the map of the lower layer of the tumulus in Kamenica, Albania. See Figure 8 for the full map.

Inconsistent results were also observed from two of the Butrint burials (1518 and 1188). The humeral cortical fragment of 1518 showed a clear sigmoidal curve for Alu, while the fibula midshaft produced signals for both DYZ1 and Alu (Figure 25). However, the Ct values for the latter were approximately ten cycles apart. Once again, this could result from contamination with male DNA or the other factors detailed above. A potential explanation for incompatible sexing results for bones of burial 1518 is the commingling of remains. Individual 1518 was buried in the same grave as 1517, mapped in Figure 34A. Figure 34B shows that the burial contained a large skeleton of an approximately 40 year old male (individual 1518), while the bone fragments at the foot of the grave (indicated by the arrow) belonged to 1517, an infant of 3 – 6 months. When the bones were first unearthed, archaeologists bagged both skeletons together (Fenton, personal communication). The bones were then rinsed with water by locals from the village of Butrint, and anthropologists later separated the remains for further analysis; it is possible that during the cleaning process bones from multiple burials were commingled, explaining the different sex results for individual 1518 (Fenton, personal communication). Alternatively remains from individual 1518 are in fact female. The humeral cortical fragment produced a clear Alu amplification curve in three replicates (data not shown) giving confidence to a female sex call. However, the DYZ1 amplification curves for the two additional replicates of the fibula midshaft were non-sigmoidal and may not be the DYZ1 product (data not shown), thereby misidentifying the remains as male.

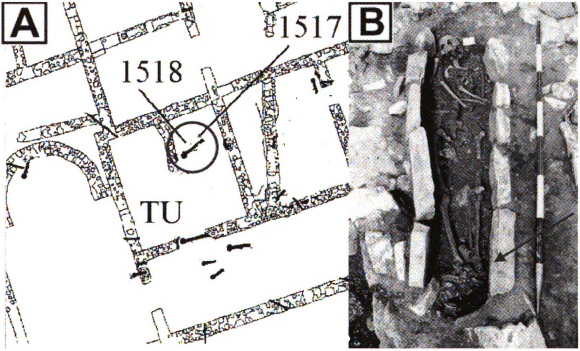

Figure 34: Map and Photograph of Burials 1518 and 1517
(A) A magnified view of burials 1518 and 1517, indicated by the circle, taken from the Butrint map (Figure 7). (B) A photograph of burials 1518 and 1517. The large skeleton is individual 1518, an estimated 40 year old male. The fragments at the foot of the grave belong to individual 1517, an infant of 3 – 6 months (arrow). (Modified from Rauzi, 2007).

Similarly, juvenile burial 1188 (Figure 32) presented a left humerus shaft that typed as female with a clear sigmoidal curve for Alu and a DYZ1 signal that did not cross the threshold, while the right petrous portion produced a signal for both loci. However, the curve for DYZ1 was not sigmoidal for either bone, bringing the male result into question. The Butrint map displayed that individual 1188 was buried along with individual 1189 (Figure 35A), and the photograph of this burial (Figure 35B) shows two skeletons present, the smaller of which is indicated by the arrow. Because of the commingling of remains, the humerus shaft or the petrous portion analyzed for burial 1188 could belong to either individual, leading to the inconsistent sexing results observed.

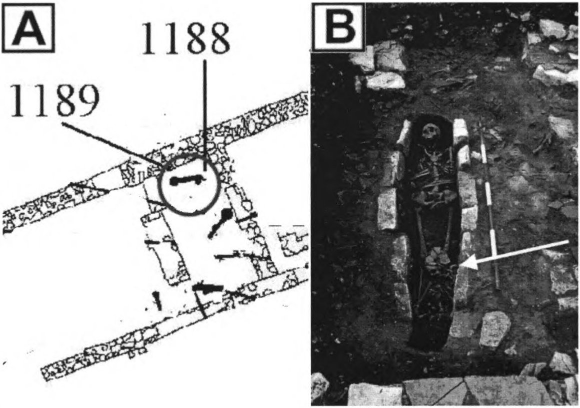

Figure 35: Map and Photograph of Burials 1188 and 1189
(A) A magnified view of burials 1188 and 1189, indicated by the circle, taken from the Butrint map from Figure 7. (B) A photograph of burials 1188 and 1189. It is unclear which skeleton belongs to either individual. The smaller skeleton is indicated by the arrow. (Modified from Rauzi, 2007).

The high sensitivity of the DYZ1/Alu assay is also its major drawback, resulting in susceptibility to contamination; however, it is possible for contamination to occur in one direction. Since Alu is present in both males and females, only DYZ1 can contaminate female DNA resulting in an incorrect sex determination, while a sexing result from contaminated male DNA would not type as female. Fortunately, DYZ1 contamination is likely to be present at only low levels, leading to an amplification curve with higher Ct values than that for Alu. How this might actually present itself could be examined by testing mixtures of female/male DNA at differing ratios to see how little male DNA is required to produce a male sexing result. Furthermore, observing the difference in Ct values for the curves at different ratios would aide in the identification of male contamination within a female sample.

There are several precautions that must be taken while using the DYZ1/Alu assay. Proper controls must be run with every set of samples to ensure that the sexing results are reliable. Both female and male control DNA must demonstrate amplification curves with Ct values that demonstrate the assay is working properly. Ideally, negative controls would show no amplification for either locus to demonstrate that the reaction solutions are not contaminated. While the Alu signal in the negative control did not affect the results of the present experiments, in a non-experimental situation one would want no amplification for both DYZ1 and Alu. In this regard, it is important to obtain reagents from suppliers with proper quality control to avoid all contamination during their production. Each reagent should be analyzed using the DYZ1/Alu assay to make sure it is free of contamination. High performance liquid chromatography purification of primers and probes may help to combat contamination as well. While setting up the assay, control DNA should be added after sample DNA, to minimize the chance of cross contamination. Furthermore, analyzing multiple DNA extractions from one piece of evidence in separate runs would help to monitor cross contamination among the samples. When sexing ancient remains with the DYZ1/Alu assay, it would be most advantageous to analyze multiple bones from an individual, thereby ensuring the accuracy of the sex determination. It is also important to become comfortable with interpreting the amplification curves of the DYZ1/Alu assay. When the curves are sigmoidal and clearly cross the threshold, it is easy to make a call. However, some results may require a certain amount of interpretation, and experience analyzing these types of data will make the sex determination simpler and more accurate.

Considering the results presented here as a whole, it is clear that the DYZ1/Alu assay outperformed the amelogenin assay with both control and forensic DNA samples. The DYZ1/Alu assay was more sensitive with low quantities of HMW and degraded DNA, more precise with DNA from hair shafts of known sex, and more accurate when sexing ancient skeletal remains. While the extreme sensitivity of the DYZ1/Alu assay may create challenges, by taking the aforementioned precautions, the assay makes an excellent tool for sexing the most challenging samples. Ultimately, this assay can assist in determining the sex of an individual for forensic investigations and anthropological research when standard sex determining methods are insufficient.

WORKS CITED

Andréasson H, Allen M. 2003. Rapid quantification and sex determination of forensic evidence materials. Journal of Forensic Sciences 48(6): 1280 – 1287.

Bailey DMD, Affara NA, Ferguson-Smith MA. 1992. The X-Y homolgous gene amelogenin maps to the short arms of both the X and Y chromosomes and is highly conserved in primates. Genomics 14: 203 – 205.

Bartha JL, Finning K, Soothill PW. 2003. Fetal Sex Determination from Maternal Blood at 6 Weeks of Gestation when at Risk for 21-Hydroxylase Deficiency. Obstetrics and Gynecology 101(5):1135 – 1136.

Bejko L, Fenton T, Foran D. 2006. Recent advances in Albanian mortuary archaeology, human osteology, and ancient DNA. In L Bejko and R Hodges (Ed.), New Directions In Albanian Archaeology: Studies presented to Muzafer Korkuti. 309 – 322. Tirana, Albania: International Centre for Albanian Archaeology.

Budowle B, Hobson DL, Smerick JB, Smith JAL. 2001. Low copy number – considerations and cautions. Proceedings of the Twelfth International Symposium on Human Identification. Madison, Wisconsin: Promega Corporation. <http://www.promega.com/geneticidproc/ussymp12proc/contents/budowle.pdf>.

Burger J, Hummel S, Herrmann B, Henke W. 1999. DNA preservation: A microsatellite-DNA study on ancient skeletal remains. Electrophoresis 20: 1722 – 1728.

Butler JM. 2007. Short tandem repeat typing technologies used in human identity testing. BioTechniques 43(4):ii – v.

Clemmer VL. 2005. Maternal relatedness within double burials of an ancient Albanian tumulus. Thesis for the Degree of M.S. School of Criminal Justice. Michigan State University.

Cox M, Mays S. 2000. Human Osteology: In Archaeology and Forensics. Cambridge University Press, New York, New York.

Edson SM, Ross JP, Cobble MD, Parsons TJ, Barritt SM. 2004. Naming the dead – confronting the realities of rapid identification of degraded skeletal remains. Forensic Science Review 16(1): 64 – 88.

Faerman M, Filon D, Kahila G, Greenblatt CL, Smith P, Oppenheim A. 1995. Sex identification of archaeological human remains based on amplification of the X and Y amelogenin alleles. Gene 167: 327 – 332.

Fenton, T. Personal communication. 2008.

Foy CA, Parkes HC. 2001. Emerging homogeneous DNA-based technologies in the clinical laboratory. Clinical Chemistry 47(6): 990 – 1000.

Graffy EA, Foran DR. 2005. A Simplified Method for Mitochondrial DNA Extraction for Head Hair Shafts. Journal of Forensic Sciences 50(5):1119 – 1122.

Graffy EA. 2003. Development and Validation of an Alkaline Extraction Method for Isolating Mitochondrial DNA from Human Hair Shafts. Thesis for the Degree of M.S. School of Criminal Justice.

Haas-Rochholz H, Weiler G. 1997. Additional primer sets for an amelogenin gene PCR-based DNA-sex test. International Journal of Legal Medicine 110: 312 – 315.

Hodges R, Bowden W, Gilkes O, Lako K. 2000. Late Roman Butrint, Albania: survey and excavations, 1994 – 98. Archeologia Medievale, XXVII: 241 – 257.

Jackson CB. 2005. A more sensitivity sex determination assay. Thesis for the Degree of M.S. School of Criminal Justice.

Kimmerle EH, Ross A, Slice D. 2008. Sexual Dimorphism in America: Geometric Morphometric Analysis of the Craniofacial Region. Journal of Forensic Sciences. 53(1):54 – 57.

Kornar DA, Potter WE. 2007. Percentage of Body Recovered and Its Effect on Identification Rates and Cause and Manner of Death Determination. Journal of Forensic Sciences. 52(3):528 – 531.

Mandrekar MN, Erickson AM, Kopp K, Krenke BE, Mandrekar PV, Nelson R, Perterson K, Shultz J, Tereba A, Westphal N. 2001. Development of human DNA quantitiation system. Croatian Medical Journal 42(3):336 – 339.

Mighell AJ, Markham AF, Robinson PA. 1997. Alu sequences. Federation of European Biochemical Society Letters 417(1):1 – 5.

Nakahori Y, Hamano K, Iwaya M, Nakagome Y. 1991. Sex identification by polymerase chain reaction using X-Y homologous primer. American Journal of Medical Genetics 39: 472 – 473.

Nesser D, Liechti-Gallati S. 1995. Sex determination of forensic samples by simultaneous PCR amplification of α-Satellite DNA from both the X and Y chromosomes. Journal of Forensic Sciences 40(2): 239 – 241.

Nicklas JA, Buel E. 2006. Simultaneous determination of total human and male DNA using a duplex real-time PCR assay. Journal of Forensic Sciences 51(5): 1005 – 1015.

Nicklas JA, Buel E. 2005. An *Alu*-based, MGB Eclipse™ real-time PCR method for quantitation of human DNA in forensic samples. Journal of Forensic Sciences 50(5): 1 – 10.

Nicklas JA, Buel E. 2003. Quantification of DNA in forensic samples. Analytical Bioanalytical Chemistry 376: 1160 – 1167.

Poinar HN. 2003. The top 10 list: criteria of authenticity for DNA from ancient and forensic samples. International Congress Series 1239: 575 – 579.

Rahman MM, Bashamboo A, Prasad A, Pathak D, Ali S. 2004. Organizational variation of DYZ1 repeat sequences on the human Y chromosome and its diagnostic potentials. DNA and Cell Biology 23(9): 561 – 571.

Rauzi CM. 2007. Genetic analysis of burials from the Butrint, Albania Triconch Palace and Merchant's House. Thesis for the Degree of M.S. School of Criminal Justice.

Rennick SL. 2005. Genetic analysis of a Mounumental Structure within the Kamenica, Albania tumulus. Thesis for the Degree of M.S. School of Criminal Justice.

Reynolds R, Varlaro J. Gender determination of forensic samples using PCR amplification of ZFX/ZFY gene sequences. Journal of Forensic Sciences 41(2): 279 – 286.

Roewer L, Arnemann J, Spurr NK, Grzeschik KH, Epplen JT. 1992. Simple repeat sequences on the human Y chromosome are equally polymorphic as their autosomal counterparts. Human Genetics 89:389 – 394.

Rozen S, Skaletsky H. 2007. Primer3 v.0.4.0. <http://frodo.wi.mit.edu/>.

Saiki RK, Gelfand DH, Stoffel S, Scharf SJ, Higuchi R, Horn GT, Mullis KB, Erlich HA. 1988. Primer-directed enzymatic amplification of DNA with a thermostable DNA polymerase. Science 239: 487 – 491.

Schmid M, Guttenbach M, Enders H, Terruhn V. 1992. A 47,XXY female with unusual genitalia. Human Genetics 90: 346 – 349.

Stacks B, Witt MM. 1996. Sex determination of dried blood stains using the polymerase chain reaction (PCR) with homologous X-Y primers of the Zinc Finger Protein Gene. Journal of Forensic Sciences 41(2): 287 – 290.

Sullivan KM, Mannucci A, Kimpton CP, Gill P. 1993. A rapid and quantitative DNA sex test: fluorescence-based PCR analysis of X-Y homologous gene amelogenin. BioTechniques 15(4):636 – 641.

Tyler-Smith C, Taylor L, Müller U. 1988. Structure of a hypervariable tandemly repeated DNA sequence on the short arm of the human Y chromosome. Journal of Molecular Biology 203:837 – 848.

Witt M, Erickson RP. 1989. A rapid method for detection of Y-chromosomal DNA from dried blood specimens by the polymerase chain reaction. Human Genetics 82: 271 – 274.